

Statistical properties of avalanches via the c -record process

Vincenzo Maria Schimmenti , Satya N. Majumdar, and Alberto Rosso
Université Paris-Saclay, CNRS, LPTMS, 91405 Orsay, France

 (Received 4 June 2021; accepted 26 October 2021; published 20 December 2021)

We study the statistics of avalanches, as a response to an applied force, undergone by a particle hopping on a one-dimensional lattice where the pinning forces at each site are independent and identically distributed (i.i.d.), each drawn from a continuous $f(x)$. The avalanches in this model correspond to the interrecord intervals in a modified record process of i.i.d. variables, defined by a single parameter $c > 0$. This parameter characterizes the record formation via the recursive process $R_k > R_{k-1} - c$, where R_k denotes the value of the k th record. We show that for $c > 0$, if $f(x)$ decays slower than an exponential for large x , the record process is nonstationary as in the standard $c = 0$ case. In contrast, if $f(x)$ has a faster than exponential tail, the record process becomes stationary and the avalanche size distribution $\pi(n)$ has a decay faster than $1/n^2$ for large n . The marginal case where $f(x)$ decays exponentially for large x exhibits a phase transition from a nonstationary phase to a stationary phase as c increases through a critical value c_{crit} . Focusing on $f(x) = e^{-x}$ (with $x \geq 0$), we show that $c_{\text{crit}} = 1$ and for $c < 1$, the record statistics is nonstationary. However, for $c > 1$, the record statistics is stationary with avalanche size distribution $\pi(n) \sim n^{-1-\lambda(c)}$ for large n . Consequently, for $c > 1$, the mean number of records up to N steps grows algebraically $\sim N^{\lambda(c)}$ for large N . Remarkably, the exponent $\lambda(c)$ depends continuously on c for $c > 1$ and is given by the unique positive root of $c = -\ln(1 - \lambda)/\lambda$. We also unveil the presence of nontrivial correlations between avalanches in the stationary phase that resemble earthquake sequences.

DOI: [10.1103/PhysRevE.104.064129](https://doi.org/10.1103/PhysRevE.104.064129)

I. INTRODUCTION

Records are ubiquitous in nature. We keep hearing about record-breaking events in sports, in stock prices, in the summer temperature in a given city, in the amount of rainfall in a given place, or in the magnitude of earthquakes in a certain geographical zone. The studies on the theory of records were initiated in the statistics literature almost 70 years ago [1–6] and since then have found numerous applications across disciplines: in sports [7–9], in the analysis of climate data [10–17], in fitness models of evolutionary biology [18–22], in condensed matter systems such as spin glasses and high temperature superconductors [23–25], and in models of growing networks [26]. Record statistics have also been studied extensively in various random walk models [27–34] with applications to avalanches and depinning of elastic lines in disordered medium [35], to the analysis of financial data [36–39], and more recently to active particles with run-and-tumble dynamics [40–42]. For reviews on record statistics in the physics literature, see Refs. [43,44].

In its most general setting, the record problem can be formulated as follows. Consider an infinite sequence of continuous random variables $\{x_1, x_2, x_3, \dots\}$ representing the entries of a discrete-time series—they may be the stock prices on successive days or the daily average temperature in a given city. The random variables are distributed via a joint distribution $P(x_1, x_2, x_3, \dots)$. A record (upper) occurs at step k if the entry x_k exceeds all previous entries, i.e., if

$$x_k > x_i, \quad \text{for all } i = 1, 2, \dots, k-1. \quad (1)$$

By convention, the first entry is always a record. The successive record values are denoted by $\{R_1, R_2, R_3, \dots\}$ and is called the associated *record series* (see Fig. 1). Furthermore, let $\{t_1, t_2, t_3, \dots\}$ denote the times at which the records occur; we will call it the associated *record-time series*. Since the first entry is always a record by convention, we have $R_1 = x_1$ and $t_1 = 1$.

Given this time series $\{x_1, x_2, x_3, \dots\}$ and its underlying probability distribution $P(x_1, x_2, x_3, \dots)$, one can investigate various observables associated to the occurrences of records. Three rather natural questions are the following:

(1) How many records M_N occur in the first N steps? For example, given the joint distribution $P(x_1, x_2, x_3, \dots)$, what is the average number of records $\langle M_N \rangle$ within the first N steps?

(2) How are the record values distributed? For example, let

$$q_k(R) = \text{Prob.}[R_k = R] \quad (2)$$

denote the probability density that the k th record (in the infinite sequence) takes value in $[R, R + dR]$. What can we say about $q_k(R)$, given the underlying joint distribution $P(x_1, x_2, x_3, \dots)$ of the original entries?

(3) Suppose that a record occurs at time t_k . How long does it take to break this record? Let $n_k = t_{k+1} - t_k$ denote the time gap between the $(k+1)$ -th record and the k th record—this is the *age* of the k th record. Let

$$\pi_k(n) = \text{Prob.}[n_k = n] \quad (3)$$

denote the distribution of the age of the k th record. Given the joint distribution of entries $P(x_1, x_2, x_3, \dots)$, can one compute $\pi_k(n)$?

i.i.d. model: The simplest model where one can compute exactly all three observables corresponds to the case when the entries x_i are *uncorrelated*, and each is drawn independently from a continuous distribution $f(x)$. In other words, the joint distribution factorizes

$$P(x_1, x_2, x_3, \dots) = f(x_1) f(x_2) f(x_3) \cdots \quad (4)$$

This is usually referred to as the independent and identically distributed (i.i.d.) model [1–6]. The probability density function (PDF) $f(x)$ is normalized to unity and its cumulative distribution is defined as $F(x) = \int_{-\infty}^x f(y) dy$. We summarize these classical results here, and for a derivation see, e.g., the review [44] with citations to the original literature [1–6].

(1) It turns out that the average number of records up to first N steps is universal, i.e., independent of $f(x)$ and is given by the simple formula

$$\langle M_N \rangle = \sum_{k=1}^N \frac{1}{k} \xrightarrow{N \rightarrow \infty} \ln N. \quad (5)$$

Thus the mean number of records grows very slowly (logarithmically) with increasing N indicating that records get increasingly harder to break. Moreover, the full distribution of M_N , i.e., $P(M, N) = \text{Prob.}(M_N = M)$ is also known and is universal. In the limit $N \rightarrow \infty$, the distribution $P(M, N)$ approaches a Gaussian form with mean $\ln N$ and variance $\ln N$.

(2) The distribution $q_k(R)$ of the value of the k th record is also known explicitly,

$$q_k(R) = f(R) \frac{[-\ln[1 - F(R)]]^{k-1}}{(k-1)!}, \quad k = 1, 2, \dots, \quad (6)$$

where $F(R)$ is the cumulative distribution. Unlike the distribution of M_N , the record value distribution $q_k(R)$ is not universal, as it depends explicitly on $f(R)$. For example, for exponentially distributed positive entries with $f(x) = e^{-x} \theta(x)$ [where the Heaviside step function $\theta(x) = 1$ if $x > 0$ and $\theta(x) = 0$ if $x \leq 0$] Eq. (6) gives

$$q_k(R) = e^{-R} \frac{R^{k-1}}{(k-1)!} \quad k = 1, 2, \dots \quad (7)$$

In this case the average record value $\langle R_k \rangle = \int_0^\infty R q_k(R) dR = k$ increases linearly with k . Similarly, the variance of R_k also grows linearly with k . In fact, for generic $f(x)$ in Eq. (6), one can show that $q_k(R)$ does not have a limiting distribution as $k \rightarrow \infty$.

(3) Finally, the age distribution $\pi_k(n)$ of the k th record is also known explicitly and turns out to be universal, i.e., independent of $f(x)$. For any $k \geq 1$, it reads [44]

$$\pi_k(n) = \sum_{m=0}^{n-1} \binom{n-1}{m} \frac{(-1)^m}{(2+m)^k} \underset{n \rightarrow \infty}{\simeq} \frac{1}{n^2} \frac{[\ln n]^{(k-1)}}{(k-1)!}. \quad (8)$$

Two important points to note for the i.i.d. model that will be important in this paper: (1) the distribution $q_k(R)$ depends on k even when $k \rightarrow \infty$, i.e., there is no limiting *stationary* record

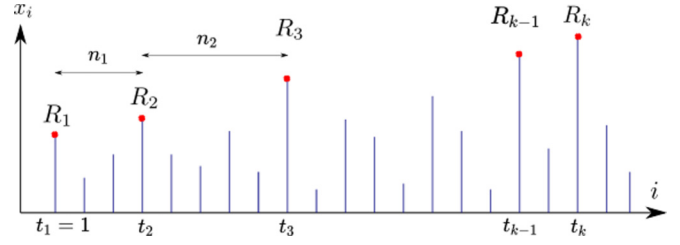


FIG. 1. An infinite discrete-time series with entries $\{x_1, x_2, \dots\}$. A record happens at step k if $x_k > x_i$ for all $i = 1, 2, \dots, k-1$. The successive record values (shown by (red) filled circles) $\{R_1, R_2, R_3, \dots\}$ form the *record series*. The times at which the records occur form a *record-time series* $\{t_1, t_2, t_3, \dots\}$. The time gap $n_k = t_{k+1} - t_k$ between the k th record and the $(k+1)$ -th record is called the *age* of the k th record. By convention, the first entry is a record, hence $R_1 = x_1$ and $t_1 = 1$.

value distribution as $k \rightarrow \infty$, simply because the record values grow with k for generic $f(x)$ and (2) similarly, the age distribution $\pi_k(n)$ in Eq. (8) also does not have a limiting stationary distribution when $k \rightarrow \infty$.

After introducing this basic background, we now turn to the main topic of this paper. Here our goal is to use the tools of record statistics to provide a simple model for the peculiar jerky motion observed in many disordered systems, as a response to an external driving force. In such systems the dynamics of the relevant degree of freedom typically alternates between static immobile states and periods of rapid motion called avalanches. Examples of such a behavior are quite ubiquitous, ranging from the crack propagation in solids [45–49], the earthquake of seismic faults [50], or the Barkhausen noise [51–53] appearing in the magnetization curve as a function of the applied magnetic field; see [54] for a review. Avalanches are well studied in the context of the depinning of an elastic interface pulled through a disordered medium by an external force [35,51,55–58]. In the absence of an external force the line is pinned by the disorder. Upon increasing the force beyond a local threshold, a portion of the interface gets depinned and its center of mass moves forward, thus creating an avalanche. Interestingly, a simple one-dimensional (1D) lattice model for depinning can be mapped exactly to the record model discussed above, as we show below.

In this lattice model, the elastic line is replaced by a single particle (representing its center of mass) that moves on an infinite 1D lattice. Under this mapping, the time series $\{x_i\}$ in Fig. 1 gets mapped on to the quenched pinning forces with the horizontal axis i labeling the sites of a 1D lattice. This defines the disorder landscape $\{x_1, x_2, \dots\}$ on which the particle moves under the effect of the applied force, $f_a(i)$ (namely, the force applied at the site i). The particle leaves the site i if $f_a(i) > x_i$. Hence, the minimal force profile allowing motion alternates between plateaus and vertical jumps (see Fig. 2). The plateaus coincide exactly with the record series $\{R_1, R_2, R_3, \dots\}$ and the vertical jumps occur exactly at the sites $\{t_1, t_2, t_3, \dots\}$ where the record occurs in Fig. 1. The age of the k th record n_k in Fig. 1 maps on to the size of the k th avalanche in the depinning model. The three observables $\langle M_N \rangle$, $q_k(R)$ and $\pi_k(n)$ have precise physical meaning in the context of depinning. For example, $\langle M_N \rangle$ is the number of

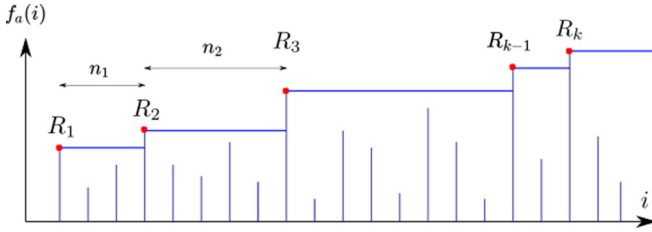


FIG. 2. The applied force profile $f_a(i)$ in the 1D depinning model has a staircase structure (shown by the solid black line), alternating between plateaus and vertical jumps. The plateau values coincide exactly with the record series $\{R_1, R_2, R_3, \dots\}$, while the jumps occur precisely at the sites where the records occur, i.e., at sites $\{t_1, t_2, t_3, \dots\}$ of Fig. 1. The age of the k th record n_k coincides exactly with the size of the k th avalanche in the depinning model.

jumps of the applied force profile in order to displace the position of the particle by N sites, given that it started at $i = 1$. Similarly, $\pi_k(n)$ represents the size distribution of the k th avalanche in the depinning model.

In the simple i.i.d. setting, the pinning forces $\{x_i\}$ in the disordered landscape are independent and identically distributed, each drawn from a continuous PDF $f(x)$. However, as we discuss in detail in Sec. II, this simple i.i.d. model, while analytically tractable, fails to reproduce the behaviors of the three observables as seen in real systems. In addition, the spatiotemporal correlations in the applied force profile $f_a(i)$ (record values) as well as in the avalanches seen in realistic systems are also not reproduced by the i.i.d. model. This calls for some amendments in this basic i.i.d. model. The idea is to introduce minimal changes in the model such that it retains its analytical tractability and yet reproduces the features observed in real systems.

After discussing briefly the previous attempts of modifying the simple i.i.d. model in Sec. II, we introduce a new model in this paper which we call the c -record model. This model has the i.i.d. landscape with input $f(x)$, and one single additional parameter $c > 0$ associated with the applied force profile $f_a(i)$. The model is precisely defined in Sec. III. We demonstrate in this paper that (a) the c -record model is exactly solvable with a rich analytical structure and (b) it reproduces qualitatively similar features for all the three observables, as well as the spatiotemporal correlations, that one observes in realistic system of depinning.

Quite remarkably, it turns out that this c -record model was already introduced in a different context in the statistics literature by Balakrishnan *et al.*, where it was called the δ -exceedance record model [59]. The parameter $\delta = -c < 0$ is negative in our context. In addition, this δ -exceedance model with a negative $\delta = -c < 0$ also appeared in the *random adaptive walk* (RAW) model to describe biological evolution on a random fitness landscape [20–22]. In fact, we use the notation c for $-\delta$ in our model following Ref. [20].

In the context of the RAW model, the two observables $\langle M_N \rangle$ and $q_k(R)$, but not $\pi_k(n)$, were already studied analytically in Ref. [20]. In the notation of Ref. [20] for RAW, our $\langle M_N \rangle$ corresponds to the mean walk length of an adaptive walker (for genome size L) $D_{\text{RAW}}(L)$ in the RAW model, with $L \sim N$ for large L . In particular, for exponentially distributed

positive fitness landscapes $f(x) = e^{-x}\theta(x)$ where $\theta(x)$ is the Heaviside step function, Ref. [20] uncovered a striking phase transition at the critical value $c = 1$, across which the asymptotic growth of $\langle M_N \rangle$, with increasing N , changes drastically.

In this paper, we revisit this c -record model in the context of depinning and avalanches. We provide a thorough analytical and numerical study of all three observables $\langle M_N \rangle$, $q_k(R)$ and $\pi_k(n)$ and also the underlying correlation structure of the record values and avalanches for a general $f(x)$, including in particular the interesting case $f(x) = e^{-x}\theta(x)$. For this particular case $f(x) = e^{-x}\theta(x)$, while our results fully agree with Ref. [20] for $c \leq 1$, we show that for $c > 1$ the model has a much richer structure than was reported in Ref. [20]. In particular, we show that for $c > 1$ and $f(x) = e^{-x}\theta(x)$, the average number of records $\langle M_N \rangle$ grows for large N as a power law

$$\langle M_N \rangle \sim N^{\lambda(c)}, \quad (9)$$

with an exponent $\lambda(c)$ that depends continuously on c (for $c > 1$) and is given by the unique positive root of the transcendental equation

$$c = -\frac{\ln(1 - \lambda)}{\lambda}. \quad (10)$$

Thus our prediction for the asymptotic growth of $\langle M_N \rangle$ in Eq. (9) for $c > 1$ differs from Ref. [20] where $\langle M_N \rangle \sim O(N)$ was reported. We also show that for $c > 1$, the record value distribution $q_k(R)$ approaches a stationary distribution as $k \rightarrow \infty$, which is given by a pure exponential behavior for all $R \geq 0$

$$q_{k \rightarrow \infty}(R) = \lambda(c) e^{-\lambda(c)R}. \quad (11)$$

In addition, the avalanche size distribution $\pi_k(n)$ also approaches a stationary distribution as $k \rightarrow \infty$ (for $c > 1$) with a power-law tail

$$\pi_{k \rightarrow \infty}(n) \sim n^{-\lambda(c)} \quad \text{as } n \rightarrow \infty, \quad (12)$$

where the exponent is the same $\lambda(c)$ as in Eq. (10).

The rest of our paper is organized as follows. In Sec. II we recall the mapping between the 1D lattice model of depinning and the record model and also discuss previously studied models that go beyond the simple i.i.d. record model. In Sec. III we define the c -record model precisely and provide a detailed summary of our results. For the particular case $f(x) = e^{-x}\theta(x)$, we also provide a detailed comparison of our results to that of Ref. [20]. In Sec. IV we set up the exact recursion relations and derive the nonlocal differential equations for the three main observables, respectively, in Secs. IV A, IV B, and IV C. In Sec. V we provide the full exact solution of all three observables in the c -record model and demonstrate the phase transition at $c = 1$. In Sec. VI we discuss in detail the criterion for stationarity of the record value distribution $q_k(R)$ as $k \rightarrow \infty$ for a stretched exponential family of $f(x)$. Section VII considers other families of $f(x)$, including an exact solution for the uniform distribution over $[0,1]$ and numerical results for the Weibull class of $f(x)$. In Sec. VIII we show some possible generalizations of the c -record process. Section IX is dedicated to the conclusion. Finally, the derivation of the asymptotic results, rather long and tedious, are relegated to Appendixes A–G.

II. DEPINNING, AVALANCHES, AND RECORD STATISTICS

To understand how record statistics of a discrete-time series, discussed in the introduction, can be used to study the avalanches associated with the depinning of an elastic interface, we consider a very simple one dimensional model where one replaces the extended interface by a point representing its center of mass [35]. The model is defined on an infinite one dimensional lattice where the lattice sites are labeled by $i = 1, 2, 3, \dots$. At each site i , we assign a positive random variable x_i , drawn independently from a continuous $f(x)$, representing the local pinning force at site i . The time series $\{x_i\}$ in Fig. 1 then defines the quenched random landscape, with the horizontal axis i labeling the lattice sites. The associated record series $\{R_1, R_2, R_3, \dots\}$ in Fig. 1 now defines the record values of this pinning force landscape. We then launch a single particle on this quenched landscape at site $i = 1$ and apply an external force f_a at site $i = 1$ that tries to drag the particle from $i = 1$ to the neighboring site $i = 2$. The force f_a is increased continuously with time at a constant rate. As long as the value of f_a is less than the local pinning force x_1 , the particle does not move from site 1. Upon increasing the force f_a , when it just exceeds $x_1 = R_1$, the particle suddenly jumps to site 2. Let $f_a(1)$ denote the applied force just when the particle leaves the site $i = 1$. The value of the applied force remains the same, i.e., $f_a = f_a(1) = x_1 = R_1$ when the particle is moving. When the particle arrives at site $i = 2$, if the current force $f_a(1)$ is less than x_2 , i.e., x_2 is a record, the particle gets stuck again at site 2 and the applied force needs to increase to exceed the pinning force x_2 . However, if x_2 is not a record, the current force $f_a(1)$ is bigger than x_2 and the particle hops from $i = 2$ to $i = 3$. Essentially the particle keeps moving forward to the right till it encounters the next record value of the landscape. We then have to increase the force f_a to exceed the current record value and the process continues. The number of sites the particle moves forward following a depinning (till it gets pinned again) is precisely the size of an avalanche.

Let $f_a(i)$ denote the value of the applied force at site i just when the particle leaves the site i . In this simple model, we thus see that the applied force profile $f_a(i)$ essentially has a staircase structure alternating between plateaus and vertical jumps (see Fig. 2). The plateau values of the force $f_a(i)$ are precisely the record values $\{R_1, R_2, R_3, \dots\}$ of the underlying landscape and the jumps of $f_a(i)$ occur exactly at the sites where records occur in the quenched landscape, i.e., they coincide with record-time series $\{t_1, t_2, t_3, \dots\}$ in Fig. 1. Consequently, the ages n_k of the records coincide exactly with the sizes of successive avalanches. Thus the three observables introduced in Fig. 1 are also very relevant in the context of depinning: (i) $\langle M_N \rangle$ measures the average number of jumps the external force has to undergo in order to displace the particle from site $i = 1$ to site $i = N$, (ii) $q_k(R)$ represents the distribution of the height of the k th plateau of the applied force, and (iii) $\pi_k(n)$ is precisely the distribution of the size of the k th avalanche.

How realistic is this simple depinning model with an i.i.d. landscape? It turns out that there are three important features in real systems that the i.i.d. model fails to reproduce faithfully:

(1) In real systems, the distribution $q_k(R)$ of the height of the k th plateau in the force profile typically approaches a stationary distribution as $k \rightarrow \infty$. In contrast, in the i.i.d. model, as seen from Eq. (6), there is no limiting stationary distribution for $q_k(R)$ as $k \rightarrow \infty$.

(2) In real systems, the avalanche size distribution $\pi_k(n)$ not only approaches a stationary distribution $\pi(n)$ as $k \rightarrow \infty$, but the stationary distribution also has a pure power-law tail, $\pi(n) \sim n^{-\tau}$ as $n \rightarrow \infty$ [52,60,61] (e.g., the celebrated Gutenberg-Richter law for earthquake magnitude). In the i.i.d. model, the result in Eq. (8) indicates that $\pi_k(n)$ neither approaches a stationary distribution as $k \rightarrow \infty$, nor does it have a pure power-law tail.

(3) Real systems exhibit very interesting correlations between the record ages, n_k , as well as between the record values, R_k . For example, after a large earthquake occurs, one observes a cascade of large aftershocks followed by long periods of quiescent activity characterized by events of small size. It turns out that in the i.i.d. model the record values R_k 's increase monotonically with k and a similar trend is observed for the ages, leaving no scope for observing cascade of events of large sizes, followed by quiescent activity.

An important improvement over the i.i.d. model is represented by the well-known Alessandro-Beatrice-Bertotti-Montorsi (ABBM) model introduced to study the avalanches in Barkhausen noise [51]. In the ABBM model, the i.i.d. landscape is replaced by a correlated one where x_i represents the position of a 1D random walk [51,54]. In this case, the avalanche size distribution $\pi_k(n)$ coincides with the return time distribution of a Brownian motion in one dimension, and hence $\pi_k(n)$ is stationary (independent of k) and does have a pure power-law tail, $\pi_k(n) \sim n^{-\tau}$ with $\tau = 3/2$. A similar analysis also follows from the study of record statistics for a random walk sequence [27]. However, in this model, $q_k(R)$ does not approach a stationary distribution as $k \rightarrow \infty$ [point (1) above] and the sequence of record ages is uncorrelated at variance with what it is seen in real systems [point (3) above].

Another modification of the simple i.i.d. record model is the so called linear-trend model [35]. In this model, the landscape of pinning forces $\{x_i\}$ remains i.i.d., but the applied force profile $f_a(i)$ changes from Fig. 2 in a simple way (see Fig. 3, upper panel). Just after the particle is deblocked from a pinning site, one assumes that the applied force $f_a(i)$ decreases linearly, $f_a(i+1) = f_a(i) - c$ (with $c > 0$) with increasing i till the particle gets blocked again. Thus, as opposed to the horizontal plateaus between two successive records in the i.i.d. model (as in Fig. 2), the force profile in the linear-trend model has a linear behavior with a negative slope, as shown schematically in Fig. 3 upper panel. The physical rationale behind the decrease of the applied force is the dissipation during the avalanche motion [in particular we have a linear decrease if $f_a(i)$ is the elastic force between the particle and a drive that moves at a constant slow rate]. In this model, at the end of an avalanche when the particle gets stuck at a new site, the force profile $f_a(i)$ jumps again to the corresponding record value of the landscape at that site and the process continues. The sequence of the force values at the beginning of an avalanche coincides with the record series $\{R_1, R_2, R_3, \dots\}$ of the landscape (see Fig. 3, upper panel).

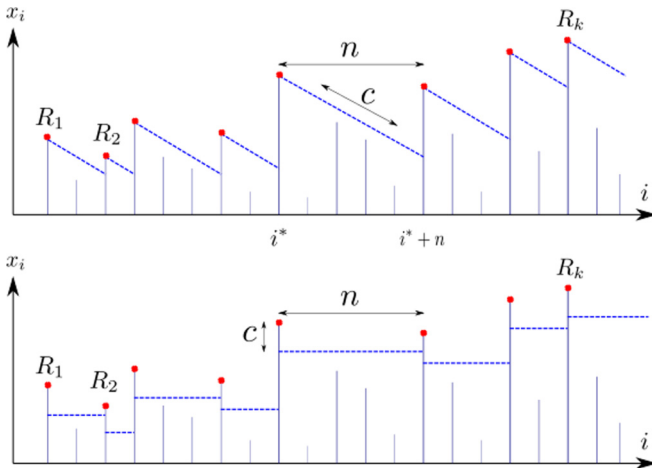


FIG. 3. Schemes for modified records. Upper panel: linear trend records. Lower panel: c -records.

Interestingly, it turns out that this linear-trend model was also introduced originally in the statistics literature by Ballerini and Resnick [62,63] and has since been studied extensively with numerous applications [64–67]. The analysis of the linear-trend model with $c > 0$ shows that the average number of records grows linearly with N for large N , i.e., $\langle M_N \rangle \approx a(c)N$ where the prefactor $a(c)$ is nontrivial and nonuniversal, i.e., depends on $f(x)$ [62,65,66]. The record value distribution $q_k(R)$ (or equivalently the distribution of the applied forces at the beginning of the k th avalanche) does approach a stationary distribution as $k \rightarrow \infty$ (as in realistic systems) that depends on the tail of $f(x)$. Similarly, the avalanche size distribution $\pi_k(n)$ also approaches a stationary distribution $\pi(n)$ as $k \rightarrow \infty$; however, this stationary distribution $\pi(n)$ does not have a power-law tail (rather an exponential cutoff) for large n as expected in real systems. In summary, the linear-trend model does reproduce some features of avalanches in realistic depinning systems, but not all.

In this paper, we introduce a simple modification of the linear-trend model, which we call the c -record model. The model is defined more precisely in the next section where we also provide a summary of our main results. This model allows exact solutions for the three observables $\langle M_N \rangle$, $q_k(R)$, and $\pi_k(n)$. We show that these observables as well as the correlation structure between records and their ages reproduce the features observed in realistic systems.

III. c -RECORD MODEL: THE DEFINITION AND A SUMMARY OF MAIN RESULTS

The model. The c -record model that we study in this paper is defined as follows. Once again, we consider an infinite i.i.d. landscape $\{x_1, x_2, x_3, \dots\}$ of quenched pinning forces defined on a 1D lattice, where each entry is chosen independently from a continuous PDF $f(x)$. Let $\{R_1, R_2, R_3, \dots\}$ denote the record series of this landscape. As in the simple i.i.d. model, the particle starts from site $i = 1$ and it can leave this site when the local applied force f_a exceeds the pinning force x_1 . The only difference in our model from that of the linear-trend model discussed in the previous section, is how the force

profile $f_a(i)$ behaves between two avalanches. In the linear-trend model, the force profile following a record decreases linearly till the next record (as in Fig. 3, upper panel). In contrast, in the c -record model, we assume that following a record, the force decreases by c only in the first step, but after that it stays flat till it encounters the next record (see Fig. 3, lower panel). More precisely, between two successive record values R_k at t_k and R_{k+1} at t_{k+1} we now have

$$f_a(i) = R_k - c, \quad \text{for } i = t_k + 1, t_k + 2, \dots, t_{k+1} - 1. \quad (13)$$

At $i = t_{k+1}$, the force $f_a(i)$ undergoes a jump to the associated record value R_{k+1} of the landscape. The physical rationale behind this new model is that the dissipation in the force profile that occurs just after depinning is short-ranged in time, e.g., occurs only during the first hopping but stays constant afterwards.

The formation of records in this c -record depinning model can be alternatively phrased in the language of standard time series discussed in the introduction. Consider, as before, an infinite i.i.d. sequence of entries $\{x_1, x_2, x_3, \dots\}$ each drawn from $f(x)$. Here a record series $\{R_1, R_2, R_3, \dots\}$ is formed recursively, in the presence of a single parameter $c > 0$, as follows. If a record occurs at some step with record value R , a subsequent entry will be a record only if its value exceeds $(R - c)\theta(R - c)$. Clearly, for $c = 0$, this is the standard record model discussed in the introduction. For $c > 0$, this is precisely the δ -*exceedance* model introduced by Balakrishnan *et al.* [59] with $\delta = -c < 0$. As already discussed in the introduction, this model with $c > 0$ was also studied in Ref. [20] as the RAW model of biological evolution in a random fitness landscape.

In this paper, we have studied the three observables $\langle M_N \rangle$, $q_k(R)$ and $\pi_k(n)$ in the c -record model, both analytically and numerically, for a class of $f(x)$'s. From the motivation of the depinning phenomenon, our main interest is to determine if, when $k \rightarrow \infty$, the c -record process becomes “stationary” or not. We say that it is stationary if the distributions $q_k(R)$ and $\pi_k(n)$ have a well-defined limit as $k \rightarrow \infty$:

$$\begin{aligned} \lim_{k \rightarrow \infty} q_k(R) &= q(R), \\ \lim_{k \rightarrow \infty} \pi_k(n) &= \pi(n). \end{aligned} \quad (14)$$

Below we summarize our main results.

The summary of main results. We find that for $c > 0$, the behavior of all three observables depends explicitly on $f(x)$ and c . For simplicity, we consider positive random variables, i.e., $f(x)$ with a positive support. In particular, three cases can be distinguished:

(1) If $f(x)$ decays slower than any exponential function as $x \rightarrow \infty$, then the record process does not reach a stationary limit for any $c > 0$, i.e., $q_k(R)$ and $\pi_k(n)$ do not have a k -independent limiting distribution as $k \rightarrow \infty$. The average number of records $\langle M_N \rangle$ grows logarithmically with N as in the standard record problem $c = 0$ (but with a different subleading constant):

$$\langle M \rangle_N = \ln N + O(1). \quad (15)$$

(2) If $f(x)$ decays faster than any exponential function as $x \rightarrow \infty$ (this includes bounded distribution), then the average

number of records grows linearly with N at the leading order:

$$\langle M \rangle_N = A_1(c)N + O(N), \quad (16)$$

where the amplitude $A_1(c)$ can be analytically determined in some cases, e.g., for uniform $f(x)$ over the interval $[0,1]$ [see Eq. (72)]. In this case, the record process also reaches a stationary limit for all $c > 0$. We compute the stationary record value distribution $q(R)$ and the stationary age distribution $\pi(n)$, analytically and numerically, in several examples of $f(R)$. In particular, for distributions with a finite support, we show that $\pi(n)$ decays exponentially with n for large n . Finally, for distributions with unbounded support and $f(x) \rightarrow e^{-x^\gamma}$ as $x \rightarrow \infty$ with $\gamma > 1$, we show that $\pi(n)$ still has a power-law tail with an exponent larger than 2.

The case $f(x) = \exp(-x)$ that separates these two behaviors turns out to be marginal, with a striking phase transition at $c = 1$. While for $0 \leq c \leq 1$, there is no limiting stationary distribution for $q_k(R)$ and $\pi_k(n)$ as $k \rightarrow \infty$, we show that for $c > 1$, they do approach stationary distributions. In particular, we find that for $c > 1$

$$q(R) = \lambda(c)e^{-\lambda(c)R}, \quad (17)$$

$$\pi(n \rightarrow \infty) = \frac{\lambda(c)[1 - \lambda(c)]}{n^{1+\lambda(c)}}, \quad (18)$$

where $\lambda(c)$ is the unique positive root of the transcendental equation:

$$c = -\frac{\ln(1 - \lambda)}{\lambda}. \quad (19)$$

The average number of records $\langle M_N \rangle$ is computed exactly in Eq. (36) and its large N behavior also exhibits a phase transition at $c = 1$. we show that

$$\langle M \rangle_N = \begin{cases} \frac{1}{1-c} \ln N - \mu(c) + O\left(\frac{1}{N}\right) & 0 \leq c < 1 \\ \ln^2 N + O(\ln N) & c = 1 \\ A_0(c)N^{\lambda(c)} + \frac{1}{1-c} \ln N + O(1) & c > 1 \end{cases}, \quad (20)$$

where the exponent $\lambda(c)$ depends continuously on c and is given in Eq. (19). Note that $\lambda(c)$ increases monotonically with increasing $c \geq 1$: $\lambda(c) \rightarrow 0$ as $c \rightarrow 1^+$, while $\lambda(c) \rightarrow 1$ only when $c \rightarrow \infty$. The explicit expression of the constant $A_0(c)$ is given in Eq. (B17). The constant $\mu(c)$ can be evaluated using the method explained in Appendix B. We also provide careful numerical checks for all our analytical formulas.

As mentioned in the introduction, precisely this marginal case $f(x) = e^{-x}$ was also studied in Ref. [20] in the context of RAW model in evolutionary biology, and indeed, this striking phase transition at $c = 1$ was already noticed there. In Ref. [20], two of the three observables, $\langle M_N \rangle$ and $q_k(R)$ [but not $\pi_k(n)$], were studied in detail, but using different notations, language, and method. In order to compare our results to those of Ref. [20], it is useful to provide a dictionary of notations for the reader. In the limit of large genome size L , the RAW model studied in [20] becomes equivalent, in the ensemble sense, to our c -record model with $N \sim L$. In this limit, our average number of records $\langle M_N \rangle$ for large N then translates to the mean length of the adaptive walk

$D_{\text{RAW}}(L \sim N)$ in [20] for large L . Furthermore, our record value distribution $q_k(R)$ is precisely $Q_{l=k}(y = R, L \rightarrow \infty)$, the probability for the adaptive walker to take $l = k$ steps to arrive at a local fitness $c(l - L) + y$ in the limit of large genome size $L \rightarrow \infty$. Hence, to summarize, for large L (or equivalently for large N in our notation)

$$N \sim L; \quad \langle M_N \rangle \equiv D_{\text{RAW}}(L \sim N), \\ q_k(R) \equiv Q_{l=k}(y = R, L \rightarrow \infty). \quad (21)$$

With the precise translation in Eq. (21) we can now compare our results with those of Ref. [20]. We start with the asymptotic large N behavior of the average number of records $\langle M_N \rangle$. For $c \leq 1$, our leading order large N results for $\langle M_N \rangle$ in Eq. (20) agree with that of Ref. [20], though the sub-leading constant $-\mu(c)$ for $0 \leq c < 1$ was not computed in [20]. However, for $c > 1$, our result in Eq. (20) is much richer (characterized by a power-law growth of $\langle M_N \rangle$ with an exponent depending continuously on the parameter c) and different from that of [20] where $\langle M_N \rangle \sim O(N)$ was reported [see Eq. (15) of [20]]. We find that the growth of $\langle M_N \rangle$ with increasing N becomes linear only when $c \rightarrow \infty$, since only in that limit $\lambda(c) \rightarrow 1$ in Eq. (20).

Next we turn to $q_k(R)$ for $c > 1$. In this case, an exact summation formula for $q_k(R)$ was derived for all c in [20] [see their Eq. (8)]. In the limit $k \rightarrow \infty$, this sum is convergent only for $c > 1$. In Ref. [20] this sum was not analyzed in the limit $k \rightarrow \infty$, since they didn't need it in their problem. In fact, it can be checked that their Eq. (8), in the limit $k \rightarrow \infty$ and for $c > 1$, satisfies the fixed-point differential equation, $q'(R) = q(R + c) - q(R)$ [see later in Eq. (42)], whose solution is precisely a single pure exponential $q(R) = \lambda(c)e^{-\lambda(c)R}$, with $\lambda(c)$ given by the positive root of Eq. (19). This is a rather nontrivial confirmation that two different methods lead to the same solution.

Let us finally conclude this summary section by mentioning that we have also studied the correlations between record values in the stationary state when it exists. In that case, the sequence of records display remarkable clustering properties (see Fig. 4, upper panel): after a large record value, we observe other large record values followed by a swarm of smaller record values. In the exponential case $f(x) = e^{-x}$, we show that the correlation between record values $\langle R_k R_{k+\tau} \rangle$ decreases exponentially with increasing τ . The value of c controls the correlation length: when $c \rightarrow 1$ from above, the correlation lengths diverges as $\sim 1/(c - 1)^2$ reminiscent of the critical phenomena (see Fig. 8, below). We also study the clustering property of record ages that correspond to avalanches (see Fig. 4, lower panel). This property is qualitatively similar to what is observed in seismic catalogs.

IV. SETTING UP THE RECURSION RELATIONS FOR THE THREE OBSERVABLES

In this section, we show how to set up the basic recursion relations to compute the three observables in the c -record model: (1) the mean number of records $\langle M_N \rangle$ up to N steps, (2) the distribution $q_k(R)$ of the value of the k th record, and (3) the distribution $\pi_k(n)$ of the time interval n_k between the k th and the $(k + 1)$ -th record. For simplicity, we will

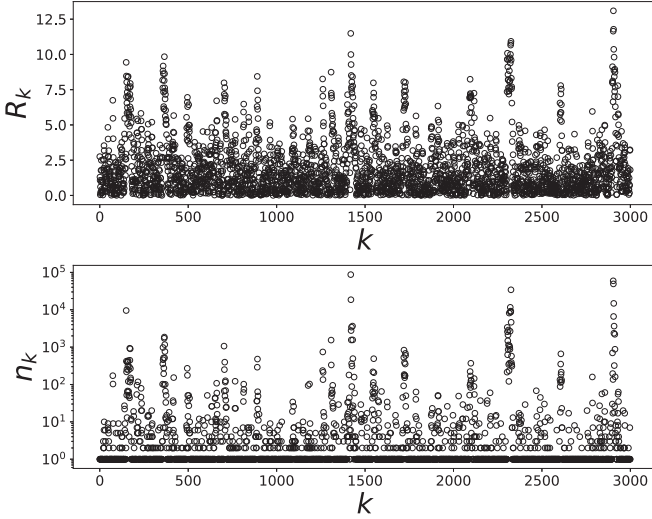


FIG. 4. Typical sequence of c -record values (upper panel) and their ages (lower panel) computed from a series of exponential number and using $c = 1.5$. Note that large record values and large ages are organized in well-defined clusters.

assume throughout that we have an infinite series of i.i.d. entries $\{x_1, x_2, x_3, \dots\}$, each drawn from a continuous $f(x)$ which has a positive support, i.e., the entries are non-negative random variables.

A. The number of records

In this subsection we derive the exact recursion relation that we have used to compute $\langle M \rangle_N$. It turns out that the main object that we need for this computation is the joint probability density $P_N(M, R_M = R)$ that in the first block of size N of the infinite series of random entries there are exactly M records and that the last record has value R . This quantity $P_N(M, R)$ satisfies a closed recursion relation

$$P_N(M, R) = P_{N-1}(M, R)\theta(R - c) \int_0^{R-c} f(x) dx + f(R) \int_0^{R+c} P_{N-1}(M-1, R') dR' \quad (22)$$

with $\theta(x)$ the Heaviside step function. It is straightforward to understand Eq. (22): the first term on the right-hand side (r.h.s.) accounts for the event when the N th entry is not a record, while the second term corresponds to the event when the N th entry is a record. In the first case, given that the last record has value R , the value of the N th entry x_N must be less than $R - c$ which happens with probability $\int_0^{R-c} f(x) dx$. In the second case, the N th entry is a record with value R , hence the previous record R' must be less than $(R + c)$ explaining the second term on the r.h.s. in Eq. (22). The recursion relation (22) starts from the initial condition

$$P_1(M, R) = \delta_{M,1} f(R), \quad (23)$$

since the first entry, by convention, is a record. The recursion relation (22), starting from (23), is nontrivial to solve since it relates $P_N(M, R)$ at R to its integral up to $R + c$ at step $N - 1$, making it a nonlocal integral equation for any $c > 0$.

In order to compute $\langle M \rangle_N$, namely, the average number of records as a function of N , we introduce $\tilde{Q}(R, z, s)$ as the double-generating function of $P_N(M, R)$:

$$\tilde{Q}(R, z, s) = \sum_{N=1}^{\infty} \sum_{M=1}^{\infty} P_N(M, R) z^N s^M. \quad (24)$$

Using Eq. (22) with the initial condition (23), we obtain the following equation for (24):

$$\tilde{Q}(R)[1 - zF(R - c)\theta(R - c)] = zsf(R) \left[1 + \int_0^{R+c} \tilde{Q}(R') dR' \right]. \quad (25)$$

For simplicity, we omitted the arguments z and s of \tilde{Q} . Evidently, Eq. (25) is also nonlocal with respect to R for any $c > 0$.

Even though the full joint distribution $P_N(M, R)$ of the number of records M and the last record value R is of interest as it contains several interesting pieces of information, we will focus on the simplest quantity, the mean number of records $\langle M \rangle_N$. To compute this, we need to extract $P_N(M)$, the distribution of the number of records M up to N steps. This is obtained by integrating over the value R of the last record up to N steps

$$P_N(M) = \int_0^{\infty} P_N(M, R) dR. \quad (26)$$

The double-generating function of $P_N(M)$ is then related to $\tilde{Q}(R, s, z)$ simply by

$$\sum_{N=1}^{\infty} \sum_{M=1}^{\infty} P_N(M) z^N s^M = \int_0^{\infty} \tilde{Q}(R, z, s) dR, \quad (27)$$

where $\tilde{Q}(R, z, s)$ is the solution of the integral equation (25). Using Eq. (27), the average number of records can be obtained from the relation

$$\begin{aligned} \langle M \rangle_N &= \sum_{M=1}^{\infty} M P_N(M) \\ &= \frac{1}{N!} \partial_z^N \partial_s \int_0^{\infty} \tilde{Q}(R, z, s) dR \Big|_{z=0, s=1}. \end{aligned} \quad (28)$$

Solving the recursion relation (25) for arbitrary $f(x)$ seems hard. However, we were able to compute \tilde{Q} and from it $\langle M \rangle_N$ explicitly for two special cases: the exponential distribution $f(x) = e^{-x} \theta(x)$ and the uniform distribution $f(x) = \mathbb{I}_{[0,1]}(x)$ with $\mathbb{I}_{[a,b]}(x)$ denoting the indicator function which is 1 if x belongs to the interval $[a, b]$ and zero otherwise.

B. The record value distribution

In this subsection we derive an exact recursion relation for the k th record value distribution $q_k(R)$ in the c -record model. We start from the joint conditional probability $q(R, n|R')$ that, given a record with value R' has occurred at some instant in the infinite sequence, the next record has value R and the age of the current record with value R' is n , i.e., there are n steps separating the current record and the next record. This

conditional probability can be very simply computed,

$$q(R, n|R') = \begin{cases} f(R) \delta_{n,1} & R' < c \\ f(R) [F(R' - c)]^{n-1} \theta(R - R' + c) & R' > c \end{cases}, \quad (29)$$

where we recall that $F(R) = \int_0^R f(y) dy$ is the cumulative distribution of each entry of the underlying time series. Equation (29) is easy to interpret: when the previous record R' is smaller than c , the very next entry with any positive value $R > 0$ will be a record, indicating that $n = 1$ is the only possible value. In contrast, when $R' > c$, assuming that there are exactly $n - 1$ entries separating two successive records with values R' and R (with $R > R' - c$), each of these intermediate entries must be less than $R' - c$ (in order that none of them is a record), explaining the factor $[F(R' - c)]^{n-1}$. The probability that the n th entry is a record is simply $f(R) \theta(R - R' + c)$. By summing over all possible age values $n \geq 1$ we obtain the distribution of the next record value conditioned on the previous one:

$$q(R|R') = \sum_{n=1}^{\infty} q(R, n|R') = f(R) \theta(c - R') + \frac{f(R)}{1 - F(R' - c)} \theta(R - R' + c) \theta(R' - c). \quad (30)$$

Equations (29) and (30) are particularly useful when simulating directly the c -record process (see Appendix G).

A recursion relation for $q_k(R)$ can then be set up using this conditional probability $q(R|R')$ as

$$q_{k+1}(R) = \int_0^{\infty} q_k(R') q(R|R') dR' = f(R) \int_0^c q_k(R') dR' + f(R) \int_c^{R+c} \frac{q_k(R')}{1 - F(R' - c)} dR', \quad (31)$$

with the initial condition $q_1(R) = f(R)$. This relation can be easily understood as follows. The first term takes into account the event when the record R' is in the range $0 \leq R' \leq c$. In this case, the entry immediately after this record is a record with probability $f(R)$. The second term on the r.h.s. in Eq. (31) accounts for the contributions coming from the case when $c \leq R' \leq R + c$. In this case, one needs to use $q(R|R')$ from Eq. (30) and integrate over all allowed values of R' . This relation (31) was also derived in [20] using different notations and for different observables, in the context of the RAW model of evolutionary biology. Furthermore, for $c = 0$, this relation was used in Ref. [13] for studying the global temperature records.

When the stationary limit of $q_k(R)$ exists, $q(R) = \lim_{k \rightarrow \infty} q_k(R)$ has to satisfy the following fixed-point equation:

$$q(R) = f(R) \int_0^c q(R') dR' + f(R) \int_c^{R+c} \frac{q(R')}{1 - F(R' - c)} dR'. \quad (32)$$

This is also a nonlocal differential equation for any $c > 0$ and is hard to solve for general $f(x)$. Again, we will see

later that for $f(x) = e^{-x} \theta(x)$ (with $c > 1$) and for the uniform distribution, it is possible to obtain explicitly the fixed-point stationary solution of Eq. (32).

C. The age distribution of records

In this subsection, we derive a recursion relation for $\pi_k(n) = \text{Prob.}(n_k = n)$ denoting the distribution of the age n_k of the k th record, in an infinite i.i.d. series. The distribution $\pi_k(n)$ can be obtained from the previously defined conditional probability $q(R, n|R')$ (29) and the record value distribution $q_k(R)$ as follows:

$$\begin{aligned} \pi_k(n) &= \int_0^{\infty} \int_0^{\infty} q(R, n|R') q_k(R') dR dR' \\ &= \delta_{n,1} \int_0^c q_k(R') dR' + \int_c^{\infty} [1 - F(R' - c)] \\ &\quad \times F^{n-1}(R' - c) q_k(R') dR', \end{aligned} \quad (33)$$

where we used $F(R' - c) = 0$ if $R' - c \leq 0$. The stationary distribution $\pi(n)$, when it exists, is obtained by taking the limit $\lim_{k \rightarrow \infty} \pi_k(n)$ and using $q(R) = \lim_{k \rightarrow \infty} q_k(R)$:

$$\begin{aligned} \pi(n) &= \delta_{n,1} \int_0^c q(R') dR' + \int_c^{\infty} [1 - F(R' - c)] \\ &\quad \times F^{n-1}(R' - c) q(R') dR'. \end{aligned} \quad (34)$$

Thus, knowing the fixed-point distribution $q(R)$ of the record value when it exists, one can compute the stationary age distribution using Eq. (34). Later we will compute $\pi(n)$ explicitly for the two solvable cases: the exponential distribution $f(x) = e^{-x} \theta(x)$ with $c > 1$ and the case of the uniform distribution over $[0, 1]$.

V. EXPONENTIAL CASE

In this section we study in detail the exponential case with $f(x) = \exp(-x) \theta(x)$.

A. Number of records

For the exponential distribution Eq. (25) reduces to

$$\begin{aligned} \tilde{Q}(R) [1 - z(1 - e^{-(R-c)}) \theta(R - c)] \\ = z s e^{-R} \left[1 + \int_0^{R+c} \tilde{Q}(R') dR' \right]. \end{aligned} \quad (35)$$

The nonlocality manifest in Eq. (25) makes it hard to find its general solution. Remarkably, for the exponential $f(x)$, this is possible. Performing a rather involved calculation, reported in Appendix A, we computed the generating function for $P_N(M)$ defined in Eq. (27). Its explicit form is given in Eq. (A10) from which we extracted the average number of records $\langle M \rangle_N$, obtaining

$$\langle M \rangle_N = N! \sum_{m=0}^{N-1} (-1)^m \frac{\prod_{k=1}^m (k-1 + e^{-kc})}{(m+1)!^2 (N-m-1)!}. \quad (36)$$

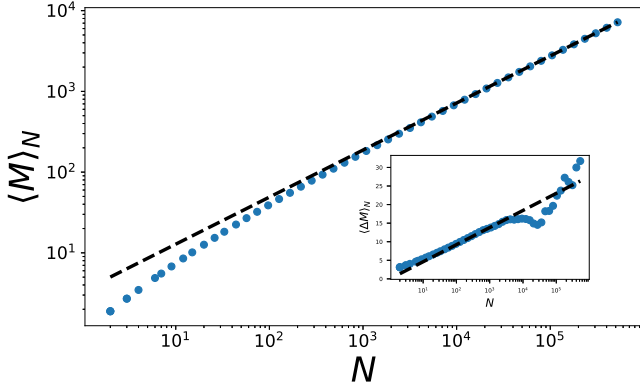


FIG. 5. Exponential case: Mean number of c -records for $c = 1.5$. Blue symbols correspond to numerical data. Black dashed line corresponds to the analytical prediction for the leading term $A_0(c)N^{\lambda(c)}$. The values of the constants are $A_0(1.5) = 3.4376$, $\lambda(1.5) = 0.5828$ [obtained from Eqs. (19) and (B17) using Mathematica]. Inset: the subleading behavior $\langle \Delta M \rangle_N = A_0(c)N^{\lambda(c)} - \langle M \rangle_N$. Black dashed line corresponds to $-\frac{1}{1-c} \ln N$.

This result for $\langle M_N \rangle$ is exact for all $N \geq 1$. For example, the first few values of N yield

$$\langle M \rangle_1 = 1, \quad (37)$$

$$\langle M \rangle_2 = 2\left(1 - \frac{1}{4}e^{-c}\right), \quad (38)$$

$$\langle M \rangle_3 = 3\left[1 - \frac{4}{9}e^{-c} + \frac{1}{18}e^{-3c}\right]. \quad (39)$$

A nontrivial check of Eq. (36) is for $c = 0$. By plugging $c = 0$ the term $\prod_{k=1}^m (k - 1 + e^{-kc})$ simplifies to $k!$. Thus Eq. (36) becomes

$$\langle M \rangle_N = \sum_{m=0}^{N-1} \binom{N}{m+1} (-1)^m \frac{1}{(m+1)}. \quad (40)$$

The above expression can be shown to coincide with the well-known result $\langle M \rangle = 1 + 1/2 + 1/3 + \dots + 1/N$. This can be done by considering the difference $\langle M \rangle_N - \langle M \rangle_{N-1}$. While the exact formula (36) is useful to compute the result for moderate values of N , the asymptotic behavior of $\langle M \rangle_N$ for large N is difficult to extract from it.

Indeed, to extract the large N behavior, we use a different approach reported in Appendix B, which leads to our main result in Eq. (20) and shows the existence of a phase transition at $c = 1$. The presence of the phase transition at $c = 1$ in the asymptotic behavior of $\langle M_N \rangle$ in Eq. (20) is also related to the fact that both $q_k(R)$ and $\pi_k(n)$ has stationary limiting distributions as $k \rightarrow \infty$, only for $c > 1$ as shown in the next Sec. VB. To check the validity of our analytical prediction we also performed direct numerical simulations using $N = 10^6$ random variables and averaging over 10^4 realizations. The results are shown in Fig. 5 for $c = 1.5$ and in Fig. 6 for $c = 0.5$, as well as for the marginal case $c = 1$. For details of the numerical simulation methods see Appendix G.

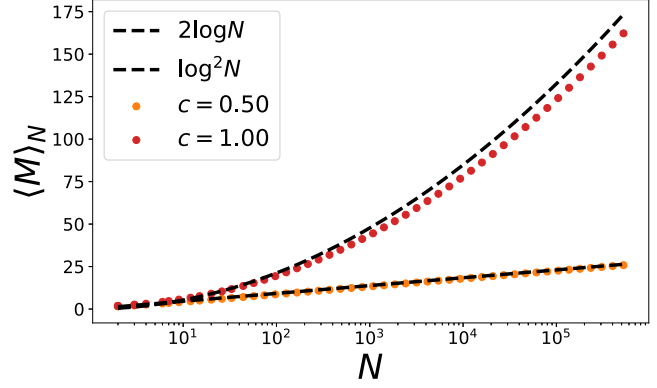


FIG. 6. Exponential case: mean number of c -records for $c = 0.5$ (red circles) and for $c = 1$ (orange circles). Circles are numerical data. Black dashed lines correspond to the analytical predictions of Eq. (20) for the leading term. For $c = 0.5$ we find $\mu(c) = 1.42878 \dots$ computed using Mathematica with the method of Appendix B.

B. Stationary record and age statistics

The solution of Eq. (31) for a given k has been studied by Park *et al.* [20] for the case $f(x) = \exp(-x)\theta(x)$. Here we focus instead on the stationary limit and we seek the solution of Eq. (32). By taking a derivative with respect to (w.r.t.) R of Eq. (32) we get

$$q'(R) = \frac{f(R)}{1 - F(R)} q(R+c) + \frac{f'(R)}{f(R)} q(R). \quad (41)$$

For the exponential case, using $f(R) = \exp(-R)$ and $1 - F(R) = \exp(-R)$, Eq. (41) reduces to

$$q'(R) = q(R+c) - q(R). \quad (42)$$

To solve this equation we use the ansatz:

$$q(R) = \lambda e^{-\lambda R}. \quad (43)$$

Equation (42) becomes

$$1 - \lambda = e^{-\lambda c}. \quad (44)$$

A positive solution for $\lambda = \lambda(c)$ exists only for $c > 1$. This means that for $c \leq 1$ there is no stationary regime. This conclusion was already pointed out in [20] based on scaling arguments and numerical simulations. Here we perform an explicit calculation which is also confirmed by the independent calculation of the large N expansion of $\langle M \rangle_N$ report in the Appendix B. The stationary average record value is $1/\lambda(c)$ (see inset of Fig. 7) and has the following limiting behaviors:

$$\langle R \rangle(c) = 1/\lambda(c) = \begin{cases} 1/2(c-1) & c \rightarrow 1^+ \\ 1 & c \rightarrow \infty \end{cases}. \quad (45)$$

The divergence as $c \rightarrow 1^+$ is one of the fingerprints of the absence of a stationary state for $c \leq 1$.

We now turn to the age distribution $\pi_k(n)$. As in the case of $q_k(R)$, a stationary distribution $\pi(n)$ in the limit $k \rightarrow \infty$ exists only for $c > 1$. For $c \leq 1$, $\pi_k(n)$ depends explicitly on k even in the $k \rightarrow \infty$ limit. To derive the stationary age distribution $\pi(n)$ for $c > 1$, we substitute $q(R)$ from Eq. (43) into Eq. (34). Upon carrying out the integration explicitly, we obtain the following exact expression of $\pi(n)$ in the stationary state valid

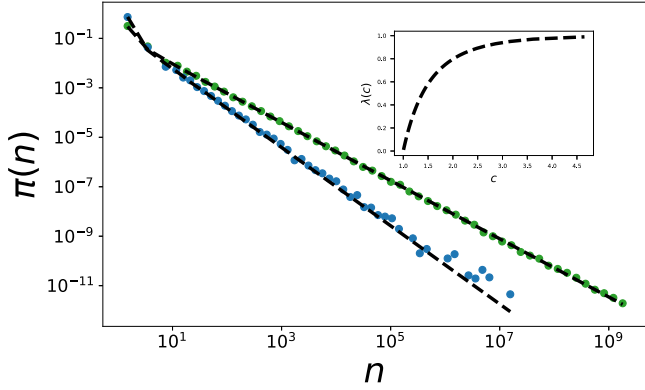


FIG. 7. Exponential case: age statistics of the stationary c -records process for $c = 1.5$ (blue circles) and for $c = 1.1$ (green circles). Numerical data are averaged over 10^4 realizations. Black dashed line corresponds to the analytical predictions of Eq. (46). The inset shows $\lambda(c)$ as a function of c .

for all $n \geq 1$ and $c > 1$:

$$\pi(n) = \lambda \delta_{n,1} + (1 - \lambda) \frac{\lambda \Gamma(n) \Gamma(\lambda + 1)}{\Gamma(n + \lambda + 1)}, \quad (46)$$

where $\Gamma(z) = \int_0^\infty e^{-x} x^{z-1} dx$ is the standard Gamma function. The stationary age (or avalanche size) distribution $\pi(n)$ is then the sum of two contributions: a delta peak at $n = 1$ and the Yule-Simon form for $n \geq 1$. Using the asymptotic behavior, $\Gamma(n)\Gamma(\alpha)/\Gamma(n + \alpha) \rightarrow 1/n^\alpha$ for large n , we unveil a beautiful power-law behavior of the stationary age distribution (see Fig. 7),

$$\pi(n \rightarrow \infty) = \frac{\lambda(1 - \lambda)}{n^{1+\lambda}}, \quad (47)$$

where $\lambda \equiv \lambda(c)$ is given by the positive root of Eq. (44) for $c > 1$. Note that the power-law exponent $(1 + \lambda(c))$ continuously varies with c . When $c \rightarrow \infty$, the exponent $\lambda(c) \rightarrow 1$, thus strengthening the amplitude of the delta peak and in addition, for large n , the power-law tail behaves as $\pi(n) \sim 1/n^2$.

We now show that the power-law decay of $\pi(n) \sim n^{-(1+\lambda(c))}$ for large n in Eq. (47) for $c > 1$ is completely consistent with the result $\langle M_N \rangle \sim N^{\lambda(c)}$ for large N in the third line of Eq. (20). To see this, we use a simple scaling argument. Given $\pi(n) \sim n^{-(1+\lambda(c))}$ for large n and the length of the series N , the mean interrecord distance (mean age of a record) scales, for large N , as

$$\langle n \rangle = \sum_{n=1}^N n \pi(n) \sim N^{1-\lambda(c)}. \quad (48)$$

Consequently, the mean number of records, which is identical to the mean number of interrecord intervals, up to step N scales for large N as

$$\langle M_N \rangle \sim \frac{N}{\langle n \rangle} \sim N^{\lambda(c)}, \quad (49)$$

which reproduces the third line of Eq. (20) for $c > 1$. In Appendix A this result is proved more rigorously.

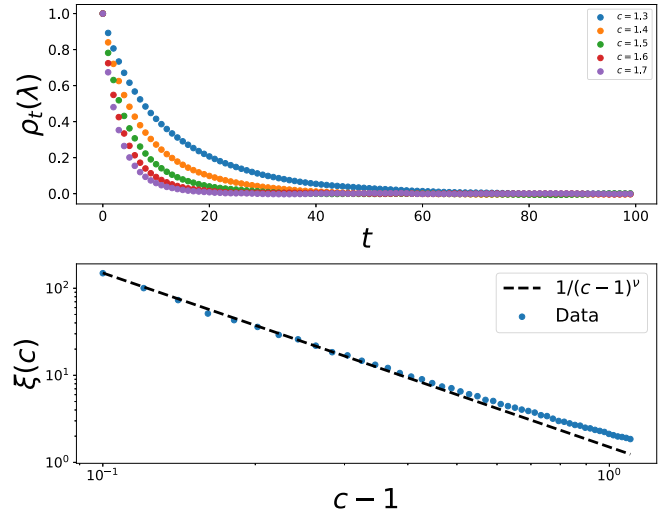


FIG. 8. Upper panel: record correlation function numerically computed as in Eq. (50). Lower panel: correlation length $\xi(c)$ as a function of $c - 1$. We fitted an exponent $\nu \approx 2$.

C. Record correlations

One of the most interesting features of the c -records statistics is shown in Fig. 4. We focus on a sequence of records when the stationary regime is already reached. The sequence tends to cluster in patterns where record values are high, followed by events of smaller value. The corresponding sequence of ages shows a similar behavior: when the record values are high we observe large ages, while the age is of the order 1 when the records are small.

To understand this behavior we can first observe that in the classical record case $c = 0$, even if there is no stationary regime, all the records values are strongly correlated. As a fingerprint of this, the sequence of record values is strictly increasing. For $c > 0$ this is not always the case. For example we know that the c -record process of an exponential series with $c > 1$ has a stationary state and the correlations have a finite range (which corresponds to the typical size of the correlated patterns in Fig. 4). To characterize this behavior we focus on the record values and study the following correlation function:

$$\rho_c(\tau) \equiv \frac{\text{Cov}(R_k R_{k+\tau})}{\text{Var}(R_k)}. \quad (50)$$

By definition $\rho_c(0) = 1$. In Appendix C we compute the correlation between two successive records, $\rho_c(1)$, which reads

$$\rho_c(1) = [1 - \lambda(c)]\{1 - \ln[1 - \lambda(c)]\}. \quad (51)$$

When $c \rightarrow \infty$, from Eq. (19), $\lambda(c) \rightarrow 1$ and $\rho_c(1) \rightarrow 0$. This means that when $c \rightarrow \infty$ the records become uncorrelated. Indeed, every random variable $\{x_1, x_2, \dots\}$ becomes a record. On the other hand as $c \rightarrow 1$, $\lambda(c) \rightarrow 0$ and $\rho_c(1) \rightarrow 1$. This result signals that the correlations are very strong, and we study numerically how fast they decay for the exponential case. In Fig. 8 we compute the correlation function (50) of a stationary record sequence for the exponential distribution and for different values of c . As in standard critical

phenomena, the correlation length diverges when one approaches the critical point $c = 1$. The numerical curves in Fig. 8 are well fitted by an exponential law as $\rho_c(\tau) = \exp[-\tau/\xi(c)]$. Using this fit we estimate the correlation length and find that it diverges as $\xi(c) \sim 1/(c - 1)^\nu$, with $\nu \approx 2$ (see Fig. 8). This result is coherent with the estimation of $\xi(c)$ via $\xi(c) \sim -1/\ln \rho_c(1)$ coming from $\exp[-1/\xi(c)] = \rho_c(1)$. Indeed as $c \rightarrow 1$, $\lambda(c) \sim 2(c - 1)$ and $-1/\ln \rho_c(1) \sim (c - 1)^{-2}$.

VI. STRETCHED EXPONENTIAL $f(x)$

Let us recall from the summary of results in Sec. III that a stationary limiting distribution for $q_k(R)$ and $\pi_k(n)$ exist for any $c > 0$, if $f(x)$ decays faster than e^{-x} for large x . In the complementary case when $f(x)$ has a slower than exponential tail, there is no stationary limiting distribution. In the borderline case $f(x) = e^{-x}$ one has a phase transition at $c = 1$, separating the nonstationary phase ($c \leq 1$) and the stationary phase ($c > 1$), as demonstrated in detail in the previous section. In this section, we will investigate the two complementary cases of $f(x)$: respectively, with a “faster” and a “slower” than exponential tail. We will do so by choosing $f(x)$ from the stretched exponential family, defined on the positive real axis $x \geq 0$,

$$f_{\text{stretched}}(x) = \frac{\gamma}{\Gamma(\frac{1}{\gamma})} e^{-x^\gamma} \quad \text{for } \gamma > 0, \quad (52)$$

with cumulative $F_{\text{stretched}}(x) = 1 - \frac{\Gamma(\frac{1}{\gamma}, x^\gamma)}{\Gamma(\frac{1}{\gamma})}$, where $\Gamma(s, t) = \int_t^\infty x^{s-1} e^{-x} dx$ the incomplete gamma function. This family of $f(x)$ in Eq. (52) includes the “borderline” exponential as the special case $\gamma = 1$. Furthermore, the case $\gamma > 1$ would correspond to a “faster” than exponential, while $\gamma < 1$ would correspond to “slower” than exponential tail.

The reason why $\gamma = 1$ is a borderline case, i.e., why the presence of a finite $c > 0$ affects the record statistics differently for $\gamma < 1$ and $\gamma > 1$ can be understood intuitively using the extreme value statistics as follows. Consider first $c = 0$. Let us consider the first N steps of the infinite i.i.d. sequence. The value of the last record in this series of size N then coincides, for $c = 0$, with the global maximum X_{max} up to N steps. For the stretched exponential $f(x)$ in Eq. (52), it is well known from the theory of extreme value statistics (for a recent review see [68]) that while the mean value $\langle X_{\text{max}} \rangle \sim (\ln N)^{1/\gamma}$ for large N , the variance scales as

$$\sigma^2 = \langle X_{\text{max}}^2 \rangle - \langle X_{\text{max}} \rangle^2 \sim (\ln N)^{2(1-\gamma)/\gamma}. \quad (53)$$

Hence, for $0 < \gamma < 1$, the width of the fluctuation grows with increasing N , while for $\gamma > 1$ it decreases for large N . Now, imagine switching on a small $c > 0$. If $0 < \gamma < 1$, an addition of a finite offset c will not affect the record statistics, since it is much smaller than the fluctuation of the record value for large N . In contrast, for $\gamma > 1$ where the width is of $O(1)$ for large N , the record value and its statistics will obviously be more sensitive to a finite offset c . The case $\gamma = 1$ is thus marginal. In fact, this change of behavior at $\gamma = 1$ for the stretched exponential family was also noticed in the asymptotic behavior of the density of near extreme events, i.e., the density of entries near the global maximum in an i.i.d. series

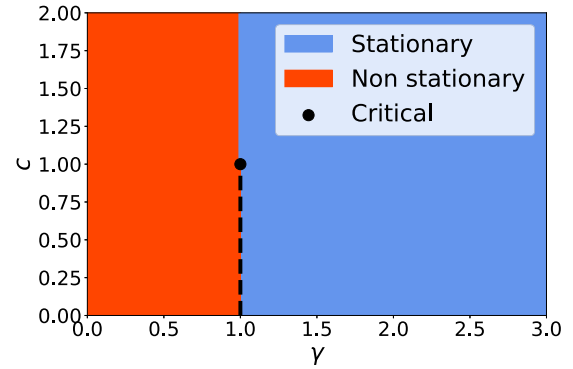


FIG. 9. Phase diagram for the stretched exponential case. For $\gamma < 1$ no stationary limit exists for any $c > 0$ while for $\gamma > 1$ it always exists. The exponential distribution $\gamma = 1$ corresponds to the marginal case, for which a stationary state exists only for $c > 1$.

[69]. Below we will provide a more precise derivation of this change of behavior in the record statistics at $\gamma = 1$ due to a nonzero $c > 0$.

In this section, for simplicity we focus only on one observable: the record value distribution $q_k(R)$. Our main goal here is to understand the criteria for having a stationary distribution for $q_k(R)$ in the limit $k \rightarrow \infty$. The other two observables $\langle M_N \rangle$ and $\pi_k(n)$ can also be studied in principle, but we will skip them here for brevity. For the c -record model with $f(x)$ belonging to this class, we then have two parameters (γ, c). Our goal is to find in which region in the ($\gamma \geq 0, c \geq 0$) quadrant, we have a stationary solution for $q_k(R) \rightarrow q(R)$ as $k \rightarrow \infty$. We will show that this leads to an interesting phase diagram shown in Fig. 9.

We start from the general recursion relation for $q_k(R)$ in Eq. (31), valid for general $f(x)$. We assume that there exists a stationary solution $q(R)$ which would then satisfy the integral equation (32). Our strategy would be to find, for $f(x)$ given in Eq. (52), if Eq. (32) allows a normalizable solution $q(R)$. If it does not, there is no stationary solution. For later analysis, it is first convenient to define

$$q(R) = f(R) G(R) \quad (54)$$

and rewrite Eq. (32) as

$$G(R) = \int_0^c G(R') f(R') dR' + \int_c^{R+c} \frac{G(R') f(R')}{1 - F(R' - c)} dR', \quad (55)$$

where we recall $F(R) = \int_0^R f(y) dy$. By taking a derivative with respect to R one gets

$$G'(R) = \frac{f(R + c)}{1 - F(R)} G(R + c). \quad (56)$$

This is a first-order nonlocal differential equation. We need only one “boundary” condition, i.e., the value of $G(R)$ at some point R , to fix the solution uniquely. To find such a condition, we note that the solution of this differential equation need, in addition, to satisfy the original integral equation (55). Substituting, e.g., $R = 0$ in Eq. (55) gives a condition

$$G(0) = \int_0^c G(R') f(R') dR'. \quad (57)$$

This shows that $G(0)$ is a constant and the solution must satisfy this condition (57) self-consistently. Another compatibility condition follows by investigating the large R limit of Eq. (55). If the limit $G(\infty)$ exists, one obtains

$$G(\infty) = \int_0^c G(R') f(R') dR' + \int_c^\infty \frac{G(R') f(R')}{1 - F(R' - c)} dR'. \quad (58)$$

For arbitrary $f(x)$, it is hard to find a general solution to Eq. (56) with boundary condition (57) or (58). Hence, below we focus on the stretched exponential class in Eq. (52), for which the first-order Eq. (56) reduces to

$$G'(R) = \frac{e^{-(R+c)^\gamma}}{\left[\int_R^\infty dR' e^{-R'^\gamma} \right]} G(R+c). \quad (59)$$

Note that for $\gamma = 1$, Eq. (59) reduces to $G'(R) = e^{-c} G(R+c)$ and this leads to the nontrivial solution $q(R) = \lambda(c) e^{-\lambda(c)R}$ for all $R \geq 0$ with $\lambda(c)$ given in Eq. (44), as discussed in the previous section.

The case $c = 0$ and arbitrary $\gamma > 0$. Let us first start with $c = 0$ case with arbitrary $\gamma > 0$. In this case, Eq. (59) becomes local in R whose general solution can be easily found,

$$G(R) = G(R_0) \frac{\int_{R_0}^\infty e^{-x^\gamma} dx}{\int_R^\infty e^{-x^\gamma} dx}, \quad (60)$$

where R_0 is arbitrary. The condition (57) says that for $c = 0$, $G(0) = 0$ identically. If we choose $R_0 = 0$ in Eq. (60), then using $G(0) = 0$, we see that the only possible solution for $G(R)$ is just $G(R) = 0$ for all R . Consequently, using Eq. (54), we get $Q(R) = 0$ which evidently cannot be normalized to unity. This indicates that there is no stationary solution $q(R)$ for $c = 0$ and arbitrary $\gamma > 0$. In other words, there is no stationary solution on the horizontal axis $c = 0$ in the phase diagram in Fig. 9.

The case $0 < \gamma < 1$ and arbitrary $c > 0$. In this case, we want to show that there is no limiting stationary solution $q(R)$ (see the red shaded region in the phase diagram in Fig. 9). In other words, we will show that a solution to Eq. (56) satisfying the condition (58) does not exist for $\gamma < 1$ with $c \geq 0$ arbitrary. To show this, it is sufficient to investigate Eq. (56) for large R , keeping $c \geq 0$ fixed. For large R , let us first assume that the limit $G(\infty)$ in Eq. (58) exists. Since $G(R)$ approaches a constant as $R \rightarrow \infty$, it follows that for any arbitrary $c \geq 0$ and large R , we must have $G(R+c) \rightarrow G(\infty)$ on the r.h.s. of Eq. (56). This gives, for large R ,

$$G'(R) \approx G(\infty) \frac{e^{-(R+c)^\gamma}}{\left[\int_R^\infty dR' e^{-R'^\gamma} \right]}. \quad (61)$$

Now consider first the large R behavior of the denominator on the r.h.s. of Eq. (61). It is easy to show that, to leading order for large R ,

$$\int_R^\infty e^{-R'^\gamma} dR' \approx \frac{1}{\gamma} R^{\gamma-1} e^{-R^\gamma}. \quad (62)$$

Substituting this in Eq. (61) one obtains for large R and for any $\gamma > 0$:

$$\begin{aligned} G'(R) &\approx G(\infty) \gamma R^{\gamma-1} e^{-(R+c)^\gamma + R^\gamma} \\ &\approx G(\infty) \gamma R^{\gamma-1} e^{-\gamma c R^{\gamma-1}}. \end{aligned} \quad (63)$$

Consider now the case $0 < \gamma < 1$. In this case, the argument of the exponential on the r.h.s. of Eq. (63) vanishes, i.e., $e^{-\gamma c R^{\gamma-1}} \rightarrow 1$ as $R \rightarrow \infty$. Consequently, integrating Eq. (63), one finds that $G(R) \sim R^\gamma$ actually grows with increasing R for $\gamma < 1$. But this is incompatible with the condition (58) and our starting assumption $G(\infty)$ is finite. In fact, this is also incompatible with the original integral equation (55). As $R \rightarrow \infty$, the l.h.s of Eq. (55) grows as R^γ , while the r.h.s. approaches a constant since the integral on the r.h.s is convergent as $R \rightarrow \infty$. Hence we conclude that for $0 < \gamma < 1$ and $c \geq 0$, there is no stationary solution for $G(R)$, and equivalently for $q(R)$ leading to the (red) shaded area of the phase diagram in Fig. 9.

The case $\gamma > 1$ and arbitrary $c > 0$. Let us first check that in this case there is no obvious incompatibility between the large R behavior in Eq. (63) and the original integral equation (55). Indeed, for $\gamma > 1$, the exponential factor $e^{-\gamma c R^{\gamma-1}}$ on the r.h.s. of Eq. (63) decays rapidly, and integrating over R we find that $G(R)$ approaches a constant as $R \rightarrow \infty$, which is perfectly compatible with Eq. (55) in the large R limit, or equivalently with Eq. (58). This already indicates that there is a normalizable stationary solution for any $c > 0$ and $\gamma > 1$. To compute explicitly this solution for arbitrary $c > 0$ (and $\gamma > 1$) still seems rather hard. Below we compute this stationary distribution for $\gamma > 1$ in two opposite limits: (1) $c \rightarrow 0^+$ and (2) $c \rightarrow \infty$ limit.

The limit $c \rightarrow 0^+$ and $\gamma > 1$ arbitrary. We start with the $c \rightarrow 0$ limit with fixed $\gamma > 1$. We fix R in Eq. (59) and take the limit $c \rightarrow 0^+$. To leading order for small c , we can approximate $G(R+c) \approx G(R)$ to make Eq. (59) local and also expand $(R+c)^\gamma \approx R^\gamma + \gamma c R^{\gamma-1}$ up to $O(c)$ with R fixed. Equation (59) then reduces to

$$\frac{1}{G(R)} \frac{dG(R)}{dR} \approx \frac{e^{-R^\gamma - c \gamma R^{\gamma-1}}}{\left[\int_R^\infty dR' e^{-R'^\gamma} \right]} \equiv g_c(R). \quad (64)$$

Note that only c -dependence appears through the factor $c \gamma R^{\gamma-1}$ inside the exponent in $g_c(R)$. For $\gamma > 1$, this term contributes significantly for large R , even when $c \rightarrow 0^+$. Hence, we cannot neglect this c -dependent term, especially for large R . One can then easily integrate Eq. (64) and obtain the solution as

$$G(R) \approx G(0) \exp \left[\int_0^R g_c(x) dx \right], \quad (65)$$

where $G(0)$ is a constant and $g_c(x)$ is defined in Eq. (64). It is easy to show that for large x , $g_c(x)$ behaves as $g_c(x) \approx \gamma x^{\gamma-1} e^{-\gamma c x^{\gamma-1}}$. Hence for $\gamma > 1$, the integral $\int_0^\infty g_c(x) dx$ is perfectly convergent and is just a constant. Consequently, we find from Eq. (65) that $G(R) \rightarrow G(\infty) = G(0) \exp[\int_0^\infty g_c(x) dx]$ as $R \rightarrow \infty$. Thus the stationary solution $q(R)$ in this $c \rightarrow 0^+$ limit is given by

$$q(R) \approx \frac{\gamma}{\Gamma(\frac{1}{\gamma})} e^{-R^\gamma} G(R) \approx f(R) G(R), \quad (66)$$

where the function $G(R)$, given in Eq. (65), is well defined for any R as long as $c \rightarrow 0^+$ (nonzero) and $\gamma > 1$. Thus, in the $c \rightarrow 0$ limit, the stationary record value distribution $q(R)$ gets modified considerably from the parent distribution $f(R)$ by the multiplicative factor $G(R)$.

The limit $c \rightarrow \infty$ and $\gamma > 1$ arbitrary. Next we consider the opposite limit $c \rightarrow \infty$. When $c \rightarrow \infty$ every random variable in the series $\{x_1, x_2, x_3, \dots\}$ is a record, hence $q(R) = f(R)$ and $G(R) = 1$ for all $R \geq 0$. Now consider c large, but not strictly infinite. In this case, the function $G(R)$ will change from its flat value $G(R) = 1$, which is valid strictly for $c \rightarrow \infty$. However, we expect that $G(R)$, in the limit $R \rightarrow \infty$, is not very sensitive to c , i.e., $G(\infty) = 1$ even for finite but large c . However, for finite but fixed R , we expect that $G(R)$ will deviate from its flat value 1. To find this change in $G(R)$ for fixed R , to leading order for large c , we can use the approximation $G(R+c) \approx 1$ on the r.h.s. of Eq. (59) and solve the resulting first-order local equation, leading to the solution

$$G(R) = 1 - \int_R^\infty \frac{e^{-(R'+c)^\gamma}}{\left[\int_{R'}^\infty e^{-x^\gamma} dx\right]} dR', \quad (67)$$

where we used the expected boundary condition $G(\infty) = 1$ mentioned above. For fixed R and large c , we can approximate $(R+c)^\gamma \approx c^\gamma + \gamma c^{\gamma-1} R$. Using this approximation in the numerator of the integrand in Eq. (67) and rescaling $z = \gamma c^{\gamma-1} R'$, we find that for $\gamma > 1$ and in the scaling limit $c \rightarrow \infty$, $R \rightarrow 0$ such that the product $c^{\gamma-1} R$ is fixed:

$$G(R) \approx 1 - \frac{e^{-c^\gamma}}{c^{\gamma-1} \Gamma\left(\frac{1}{\gamma}\right)} e^{-\gamma c^{\gamma-1} R}. \quad (68)$$

This is clearly compatible with the starting ansatz that $G(\infty) = 1$. Finally, using this in Eq. (54) we get the stationary solution for $\gamma > 1$ and large c limit:

$$q(R) \approx f(R) \left[1 - \frac{e^{-c^\gamma}}{c^{\gamma-1} \Gamma\left(\frac{1}{\gamma}\right)} e^{-\gamma c^{\gamma-1} R} \right]. \quad (69)$$

Thus, in the $c \rightarrow \infty$ limit, $q(R)$ approaches $f(R)$ with a small additive correction term as given in Eq. (69).

Summarizing, for $\gamma > 1$ in the phase diagram in Fig. 9, the record value distribution becomes stationary for large k , for any $c > 0$. In the two limits $c \rightarrow 0$ and $c \rightarrow \infty$, the stationary distribution $q(R)$ is given, respectively, in Eqs. (66) and (69). We have checked these results numerically in Fig. 10 for $\gamma = 2$. In this figure, we see that as c increases, $q(R)$ progressively approaches $f(R)$.

We have also computed numerically the mean number of records $\langle M_N \rangle$ up to N steps. As indicated in the phase diagram in Fig. 9, we expect that for $0 < \gamma < 1$ the record process is nonstationary, i.e., the effect of c is insignificant and the system behaves similar to $c = 0$. Hence in this regime (red shaded region in the phase diagram in Fig. 9, we expect $\langle M_N \rangle \simeq \ln N$ for large N , for any $c > 0$. This prediction is verified numerically in Fig. 11, for $\gamma = 1/2$ and for several values of c . In contrast, for $\gamma > 1$ and $c > 0$ (blue shaded region in the phase diagram in Fig. 9), we have a stationary phase. In this case, we expect a linear growth $\langle M_N \rangle \simeq A_1(c) N$ for large N , with an c -dependent amplitude $A_1(c) \leq 1$. In the limit $c \rightarrow \infty$, we expect $A_1(c) \rightarrow 1$, since every entry

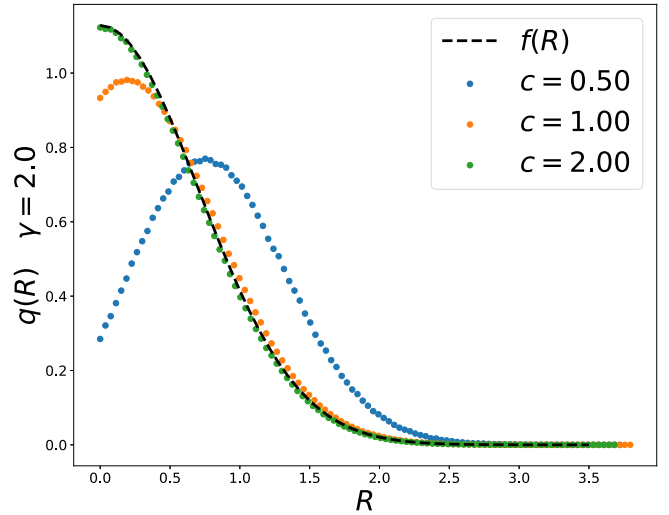


FIG. 10. Stretched exponential case: stationary record distributions $q(R)$ at $\gamma = 2$ and for different c . As c gets bigger, $q(R)$ approaches $f(R)$.

becomes a record in this limit. In Fig. 12 we verify this prediction for fixed $\gamma = 2$ and for several values of c .

VII. OTHER DISTRIBUTIONS

In this section, we study other classes of $f(x)$. First, we consider the uniform distribution of $f(x)$ over the bounded interval $[0,1]$ for which we present exact analytical results for all three observables $\langle M_N \rangle$, $q_k(R)$, and $\pi_k(n)$. We then consider more general bounded distributions. Bounded distributions belong to the family of $f(x)$ with a “faster than” exponential tail, hence we anticipate and demonstrate below that both $q_k(R)$ and $\pi_k(n)$ allow stationary limiting distributions as $k \rightarrow \infty$ for bounded $f(x)$. We then consider another class of unbounded distribution, which we call the Weibull class

$$f_{\text{Weibull}}(x) = \gamma x^{\gamma-1} e^{-x^\gamma} \quad \text{for } \gamma > 0 \quad (70)$$

with $F_{\text{Weibull}}(x) = 1 - e^{-x^\gamma}$. It turns out that this $f(x)$ is easier to sample numerically using the inverse Transform method,

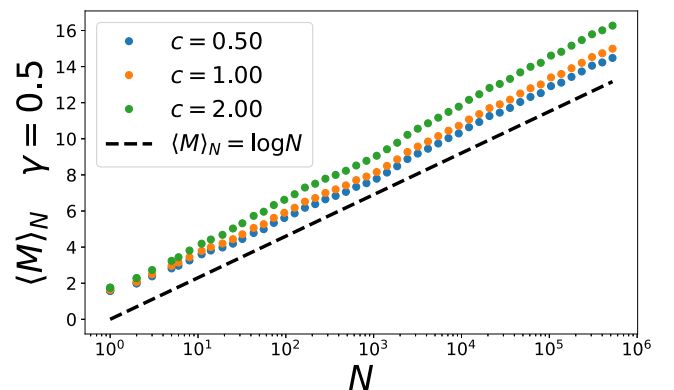


FIG. 11. Stretched exponential case: logarithmic growth of the mean number of c -records for different c and $\gamma = 0.50$. The dashed line is a guide to the eye.

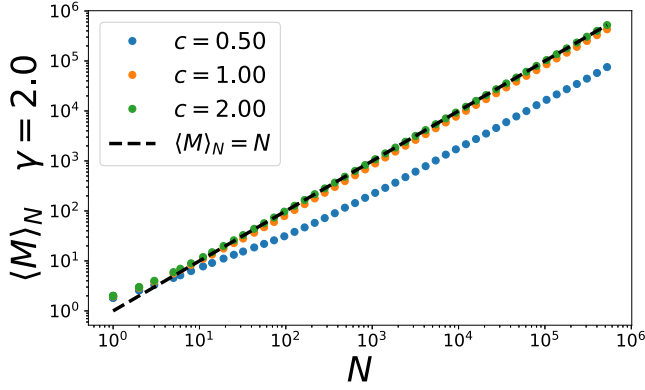


FIG. 12. Stretched exponential case: linear growth of the mean number of c -records for different c and $\gamma = 2$.

as explained in Appendix G. We present detailed numerical results for all three observables $\langle M_N \rangle$, $q_k(R)$ and $\pi_k(n)$ for this case.

A. Bounded distributions

The c -record process associated to i.i.d. time series drawn from bounded distributions has a well-defined stationary limit for any $c > 0$. For simplicity we restrict the interval to the segment $[0,1]$. This implies that for any $c > 1$, every entry x_i of the time series is a record.

B. Uniform distribution

We first consider the uniform distribution $f(x) = \mathbb{I}_{[0,1]}(x)$ and show that the mean number of records, the stationary record distribution and their age distribution can be explicitly computed for $1/2 \leq c \leq 1$. For $0 < c < 1/2$, the calculations are more cumbersome and we rely on Monte Carlo simulations.

To compute the mean number of records we study Eq. (25) for the uniform distribution. Its expression simplifies to

$$\begin{aligned} \tilde{Q}(R)[1 - z(R - c)\theta(R - c)] \\ = z s + z s \int_0^{\min(1, R+c)} \tilde{Q}(R') dR'. \end{aligned} \quad (71)$$

This equation is solved in Appendix D for $1/2 \leq c \leq 1$ and the exact mean number of records reads

$$\langle M \rangle_N = [2 - c + \ln(c)]N + \frac{1 - c}{c} + \ln(c). \quad (72)$$

Note that when $c = 1$, we get $\langle M \rangle_N = N$ as expected. In Fig. 13 we numerically computed $\langle M \rangle_N$ for different values of c and included the analytical predictions for $1/2 \leq c \leq 1/2$.

The stationary record distribution $q(R)$ satisfies Eq. (41) together with the condition that $q(R) = 0$ for $R > 1$:

$$q'(R) = \begin{cases} 0 & 1 - c < R < 1 \\ \frac{q(R+c)}{1-R} & 0 < R < 1 - c \end{cases}. \quad (73)$$

Equation (73) is valid for any $0 \leq c \leq 1$. For $c \geq 1/2$, it can be simply solved. In particular, imposing the global

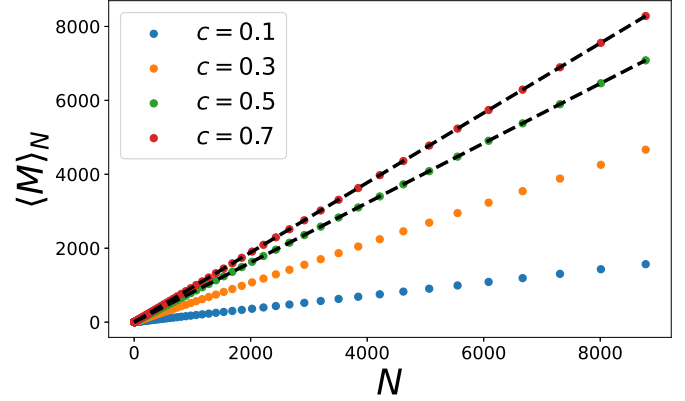


FIG. 13. Uniform case: mean number of c -records for different c . For $c \geq 1/2$ we include the analytical predictions in Eq. (72) as shown by dashed lines. The agreement is excellent.

normalization, one gets

$$q(R) = \frac{1}{2 - c + \ln(c)} \begin{cases} 1 & 1 - c < R < 1 \\ 1 - \ln \frac{1-R}{c} & 0 < R < 1 - c \end{cases}. \quad (74)$$

In Fig. 14 (upper panel) we show $q(R)$ for different values of c along with the analytical predictions for $1/2 \leq c \leq 1$.

The stationary age distribution $\pi(n)$ (for $1/2 \leq c \leq 1$) follows from Eqs. (34) and (74):

$$\begin{aligned} \pi(n) = \frac{1 + \ln(c)}{2 + \ln(c) - c} \delta_{n,1} \\ + \frac{1}{2 + \ln(c) - c} \frac{(1 - c)^n}{n} \left[1 - \frac{n(1 - c)}{n + 1} \right]. \end{aligned} \quad (75)$$

$\pi(n)$ shows a delta peak at $n = 1$, as in the exponential case. For large n , $\pi(n)$ decays exponentially over a characteristic scale $-1/\ln(1 - c)$ that gets smaller as $c \rightarrow 1$. The fact that $\pi(n)$ has a well-defined first moment is compatible with the

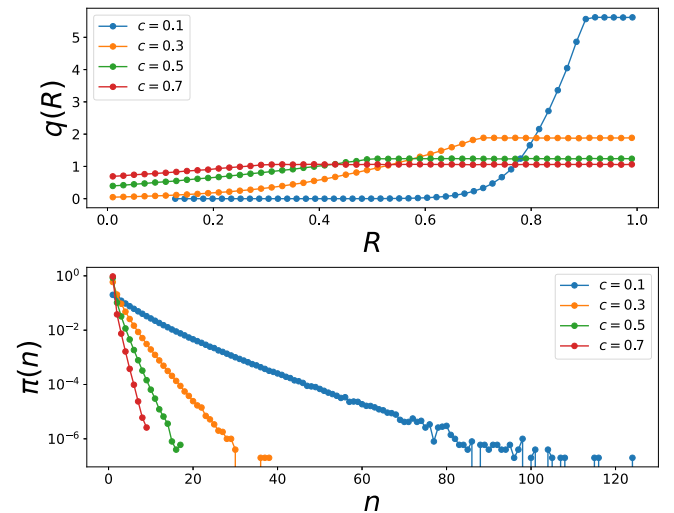


FIG. 14. Record (upper panel) and age (lower panel) distributions for various c for the uniform distribution. Analytical results of Eqs. (74) and (75) are shown by solid lines in the upper panel.

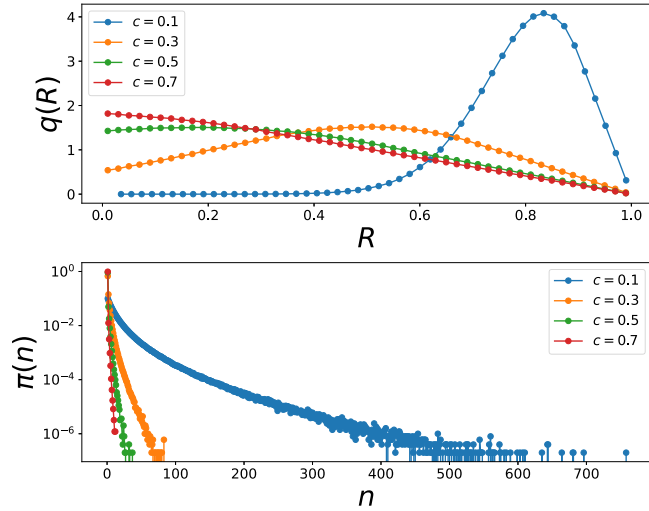


FIG. 15. Record (upper panel) and ages (lower panel) distributions for various c for the bounded case with cumulative distribution $F(x) = 1 - (1 - x)^2$ with $0 \leq x \leq 1$.

scaling of the average number of records, namely, $\langle M \rangle_N \propto N$ as $N \rightarrow \infty$.

C. Generic bounded distributions

The c -record process associated to a generic bounded distribution is more difficult to characterize analytically. However, some of the features that we found for the case of the uniform distribution remain valid. In particular for any value of c the mean number of records grows linearly with N (at large N) and the stationary distribution of ages displays an exponential cutoff. As an illustration we studied numerically the family of distribution with cumulative $F(x) = 1 - (1 - x)^\nu$. The uniform distribution corresponds to $\nu = 1$. In Fig. 15 we report our results for $\nu = 2$: in the upper panel the study of the stationary record distribution $q(R)$ and in the lower panel the age distribution $\pi(n)$.

D. Numerical results for the Weibull family

In this section we briefly summarize the numerical results for $\langle M \rangle_N$, $q(R)$, $\pi(n)$ for the Weibull family. In Fig. 16 we show the mean number of records $\langle M \rangle_N$ as a function of N for 10^3 realizations of the c -record process. For large enough N the scaling $\langle M \rangle_N \propto N$ is recovered. In Fig. 17 we show the stationary record distribution for the Weibull distribution at $\gamma = 2$. We find a stationary distribution for any $c > 0$. As c gets bigger, $q(R)$ approaches $f(R)$, as expected. In Fig. 18 we show the average record $\langle R \rangle_\gamma(c)$ as a function of c for different γ . We also insert the scaling as $c \rightarrow 0^+$ of the average record value obtained using the argument in Appendix F:

$$\langle R \rangle_\gamma(c) \approx (c\gamma)^{\frac{1}{\gamma-1}}. \quad (76)$$

Finally Fig. 19 shows the age of record distributions at $\gamma = 2$ for different values of c . The distributions have a power-law decay as $n \rightarrow \infty$ with an exponent $\tau \geq 2$: $\pi(n) \sim n^{-\tau}$. This numerical result is compatible with the scaling $\langle M \rangle_N \propto N$ of

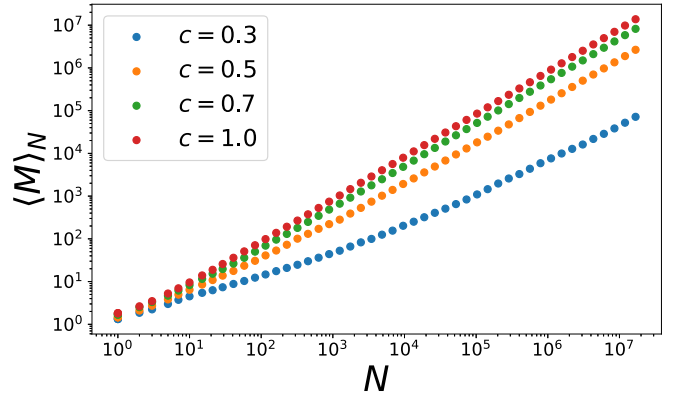


FIG. 16. Weibull case with $\gamma = 2$ mean number of c -records for various c . As c gets smaller the convergence to $\langle M \rangle_N \propto N$ gets slower.

the average number of records since a power law with $\tau \geq 2$ has a well-defined first moment.

VIII. GENERALIZATIONS OF THE RECORD PROCESS

Before the conclusion we would like to discuss some possible generalizations of the c -record problem. For simplicity here we focus only on the conditions for the existence of a stationary record distribution and on its form. We let the calculations of the mean number of records and of the age statistics to future works. A few protocols can be considered as a straightforward generalization of the c -record process:

(1) The constant c can be promoted to be a positive random variable with distribution $g(c)$. For $f(x) = e^{-x}\theta(x)$ the fixed-point equation for the stationary record distribution, averaged over all possible values of c (annealed average), writes

$$q'(R) = \int_0^\infty g(c)q(R+c)dc - q(R). \quad (77)$$

Remarkably this equation admits an exponential solution $q(R) = \lambda e^{-\lambda R}$ if the equation

$$1 - \lambda = \tilde{g}(\lambda) \equiv \int_0^\infty e^{-\lambda c} g(c) dc \quad (78)$$

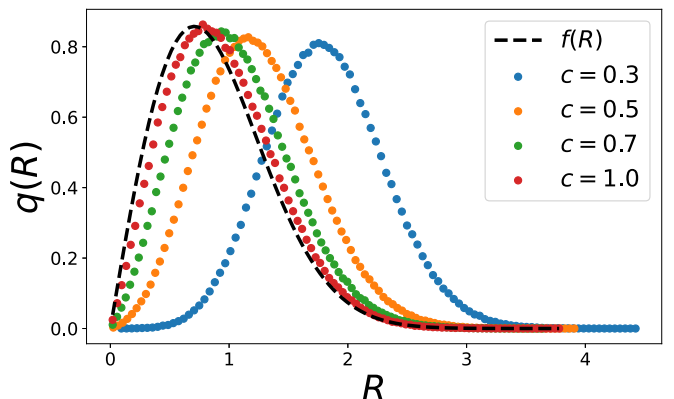


FIG. 17. Record distributions for the Weibull family with $\gamma = 2$ for various c .

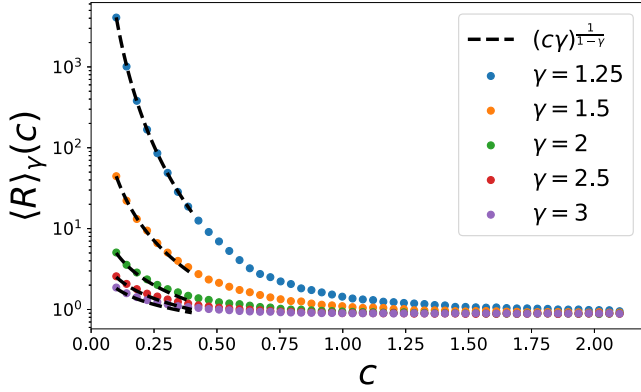


FIG. 18. Average record value for various γ and c for the Weibull family. We plot with the dashed black line the expected scaling of the average for $c \rightarrow 0^+$ [see Eq. (76)].

has a positive solution λ . For example if $g(c)$ is an exponential distribution, a stationary state is reached if its mean is bigger than 1.

(2) The definition of the c -record can be extended with a function $c(R)$, namely, R_k is a record if $R_k > R_{k-1} - c(R_{k-1})$. As a concrete example one can consider $c(R) = cR$ with $c < 1$ (for $c \geq 1$ all the values of the time series are records):

$$R_k > (1 - c)R_{k-1}. \quad (79)$$

The fixed-point equation for the stationary record distribution $q(R)$ satisfies

$$q'(R) = \frac{f(R)}{1 - F(R)} \frac{1}{1 - c} q\left(\frac{R}{1 - c}\right) + \frac{f'(R)}{f(R)} q(R). \quad (80)$$

Equation (80) becomes simple for a Pareto distribution $f(x) = \frac{\alpha}{x^{\alpha+1}}\theta(x - 1)$:

$$q'(R) = \frac{\alpha}{R(1 - c)} q\left(\frac{R}{1 - c}\right) - \frac{\alpha + 1}{R} q(R). \quad (81)$$

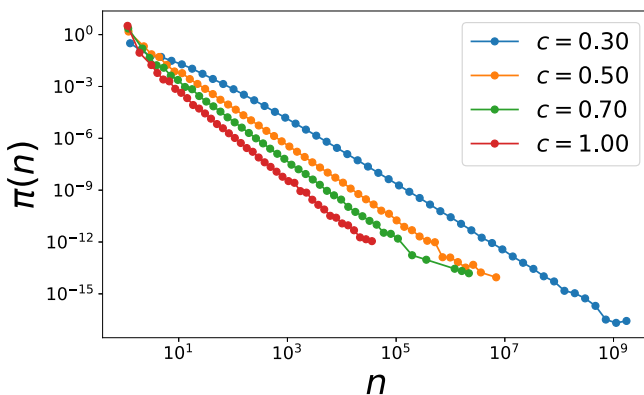


FIG. 19. Age of record numerical distributions for the Weibull family at $\gamma = 2$ and varying c . All the distributions show a power-law tail with exponent ≥ 2 .

The stationary state exists for $c > 1 - e^{-\frac{1}{\alpha}}$ and the solution of (81) still a Pareto distribution $q(R) = \frac{\beta}{R^{\beta+1}}\theta(R - 1)$ with β the unique positive solution of the transcendental equation

$$1 - \frac{\beta}{\alpha} = (1 - c)^\beta. \quad (82)$$

The records generated by this process are equivalent to the c -records discussed in this paper via the map $R_k \rightarrow \ln R_k$. Under this mapping the Pareto distribution becomes the exponential distribution.

(3) Finally we consider the k -dependent record condition

$$R_k > R_{k-1} - c(k + 1)^{b-1} \quad (83)$$

for a constant $b > 0$. This protocol has been considered in [22] in the context of evolutionary biology: the quantity $c(k + 1)^{b-1}$ is called *handicap* and the analysis is carried out for both increasing $b > 1$ and decreasing $b < 1$ handicaps. The case $b = 1$ coincides with the c -record process. We refer the reader to the original work [22] for details.

IX. CONCLUSION

In this paper, we have shown that a simple record model of an i.i.d. series, which we call the c -record model, can be successfully used to understand and explain several realistic features of avalanche statistics in disordered systems, an example being the earthquake dynamics in seismicity. This model has a single parameter $c \geq 0$ and the other input is the distribution $f(x)$ of an entry. We have focused on three natural observables: (1) the mean number of records $\langle M_N \rangle$ up to step N in an infinite series, (2) the distribution $q_k(R)$ of the value of the k th record and, (3) the distribution $\pi_k(n)$ of the time interval n between the k th and the $(k + 1)$ -th record.

One of our main conclusions is that if $f(x)$ decays, for large x , slower than an exponential, both $q_k(R)$ and $\pi_k(n)$ do not have stationary limits as $k \rightarrow \infty$ and $\langle M_N \rangle \sim \ln N$ for large N , as in the $c = 0$ case. Thus the effect of c is not very significant for $f(x)$ with a slower than exponential tail. In contrast, if $f(x)$ has a faster than exponential tail, both $q_k(R) \rightarrow q(R)$ and $\pi_k(n) \rightarrow \pi(n)$ approach stationary limiting forms as $k \rightarrow \infty$. In particular, we show that $\pi(n)$ decays faster than $1/n^2$ for large n (indicating that $\langle n \rangle$ is finite). Additionally, in this case, the mean number of records grows linearly as $\langle M_N \rangle \sim A_1(c)N$ for large N with $A_1(c) \leq 1$. Thus, for $f(x)$ decaying faster than exponential, the statistics of these three observables for finite c are fundamentally different from the standard $c = 0$ case. When $f(x)$ has an exponential tail, it turns out to be a marginal case where there is a phase transition at a critical value c_{crit} . For $c < c_{\text{crit}}$, the observables have qualitatively similar behavior as the $c = 0$ case. In contrast for $c > c_{\text{crit}}$, both $q_k(R)$ and $\pi_k(n)$ have stationary limits as $k \rightarrow \infty$. We have illustrated by an explicit calculation for $f(x) = e^{-x}\theta(x)$ for which $c_{\text{crit}} = 1$. In this case we have shown that for $c > 1$, the stationary avalanche size distribution $\pi(n) \sim n^{-1-\lambda(c)}$ has a power-law tail for large n with $\lambda(c) \leq 1$, indicating that the first moment diverges. Remarkably, the exponent $\lambda(c)$ depends continuously on c and is given by the root of the transcendental equation, $c = -\ln(1 - \lambda)/\lambda$. We have also computed exactly the stationary

record value distribution $q(R)$ for $c > 1$ and shown that it is a pure exponential, $q(R) = \lambda(c) e^{-\lambda(c)R}$, for all $R \geq 0$.

An important feature of this c -record model is a nontrivial correlation structure between record values, as well as between record intervals. In this paper we have explored only partially this structure, and it would be interesting to characterize this correlation structure in a more complete fashion.

We have also provided some generalizations of this simple c -record model, where the criteria for record formation, i.e., the offset c_k depends on the record value R_k as well as on the record index k . In all these cases, the offset c_k remains constant (albeit k -dependent) as in the lower panel of Fig. 3. Previously, the linear trend model was studied where the offset decreases linearly with time during an avalanche (as in the upper panel of Fig. 3). One can then ask how the record statistics gets modified for a general decreasing offset function during an avalanche.

Finally, in this paper, we have considered a series of i.i.d. variables as a model for the pinning force landscape. It is natural to consider a model where the landscape is correlated. For example, in the ABBM model, the entries of the series correspond to the positions of a random walker. This remains a challenging open problem.

ACKNOWLEDGMENTS

We thank O. Giraud for an illuminating discussion. We acknowledge F. Landes, E. Lippiello, J. Krug, S.-C. Park, and G. Petrillo for useful discussions. We acknowledge 80 Prime CNRS support for the project CorrQuake.

APPENDIX A: EXPONENTIAL CASE: $P_N(M, R)$

Our starting point is Eq. (35) for the generating function $\tilde{Q}(R)$ in the exponential case, $f(x) = e^{-x} \theta(x)$. We solve it in terms of $H(R) = \int_0^R \tilde{Q}(R') dR'$. Thus Eq. (35) becomes

$$H'(R)[1 - z(1 - e^{-(R-c)})\theta(R-c)] = z s e^{-R} [1 + H(R+c)]. \quad (\text{A1})$$

The initial condition for $H(R)$ is $H(0) = 0$. In order to solve (A1) we need to distinguish region I with $R < c$, region II with $R > c$, and match the two solutions at $R = c$. We call $H_I(R)$ the solution for region I and $H_{II}(R)$ the one for region II.

We start with region II ($R > c$) and use the ansatz

$$H_{II}(R) = \sum_{m=0}^{\infty} a_m e^{-mR}. \quad (\text{A2})$$

Substituting this in Eq. (A1) and matching terms of e^{-R} on both sides, we get the following recursion relation for the coefficients a_m :

$$a_1 = -\frac{zs}{1-z}(1+a_0), \quad (\text{A3})$$

$$a_m = -\frac{ze^c}{1-z} \left(\frac{m-1+se^{-mc}}{m} \right) a_{m-1}. \quad (\text{A4})$$

By iterating we get

$$a_m = (-1)^m \left(\frac{ze^c}{1-z} \right)^m \frac{1}{m!} b_m(s) (1+a_0), \quad (\text{A5})$$

where

$$b_m(s) = \begin{cases} \prod_{k=1}^m (k-1+se^{-kc}) & m \geq 1 \\ 1 & m = 0 \end{cases}. \quad (\text{A6})$$

We then rewrite $H_{II}(R)$ as

$$H_{II}(R) = (1+a_0) \sum_{m=0}^{\infty} \left(-\frac{ze^c}{1-z} \right)^m \frac{b_m(s)}{m!} e^{-mR}. \quad (\text{A7})$$

The coefficient a_0 is a parameter that must be set by imposing the matching of $H_I(R)$ and $H_{II}(R)$ at $R = c$. In region I, $H_I(R)$ satisfies

$$(1-z) \frac{dH_I(R)}{dR} = z s e^{-R} [1 + H_{II}(R+c)]. \quad (\text{A8})$$

Substituting the solution of $H_{II}(R)$ from Eq. (A7) on the r.h.s. of (A8) and solving the first-order equation for $H_I(R)$, using $H_I(0) = 0$, gives

$$H_I(R) = sz(1+a_0) \sum_{m=0}^{\infty} \left(-\frac{z}{1-z} \right)^m \frac{b_m(s)}{(m+1)!} \frac{(1-e^{-(m+1)R})}{m+1}. \quad (\text{A9})$$

The continuity at $R = c$, namely $H_I(c) = H_{II}(c)$, fixes a_0 :

$$a_0 = \frac{1}{\sum_{m=0}^{\infty} \left(-\frac{z}{1-z} \right)^m \frac{b_m(s)}{m!} \left(1 - \frac{zs(1-e^{-(m+1)c})}{m+1} \right)} - 1. \quad (\text{A10})$$

In the limit $R \rightarrow \infty$, we have $H(\infty) = \int_0^{\infty} \tilde{Q}(R') dR'$. On the other hand, it follows by taking $R \rightarrow \infty$ limit in Eq. (A2) that $H(\infty) = a_0$. Combining these two and using Eq. (27), we finally identify

$$\sum_{N=1}^{\infty} \sum_{M=1}^{\infty} P_N(M) z^N s^M = a_0 = a_0(z, s), \quad (\text{A11})$$

with a_0 given in Eq. (A10). One can check that for $c = 0$

$$a_0 = \frac{1}{(1-z)^s} - 1, \quad (\text{A12})$$

which reproduces the well-known result for the generating function of the standard record process [44]. To find the generating function of $(M)_N$ one must study a_0 in the vicinity of $s = 1$. The expansion around $s = 1$ from (A10) is not straightforward. We want to rewrite the denominator of a_0 in a simpler form using $\tilde{b}(x, s)$, the generating function of $b_m(s)$. We first introduce an useful identity:

$$\begin{aligned} \tilde{b}(x, s) &= \sum_{m=0}^{\infty} \frac{b_m(s)}{m!} x^m \\ &= 1 + \sum_{m=1}^{\infty} (m-1+se^{-mc}) \frac{b_{m-1}(s)}{m!} x^m \\ &= 1 + \sum_{m=1}^{\infty} \frac{b_{m-1}(s)x^m}{(m-1)!} - \sum_{m=1}^{\infty} \frac{b_{m-1}x^m}{m!} \\ &\quad + s \sum_{m=1}^{\infty} \frac{b_{m-1}(xe^{-c})^m}{m!} \end{aligned}$$

$$= 1 + x\tilde{b}(x, s) - \sum_{m=1}^{\infty} \frac{b_{m-1}x^m}{m!} + s \sum_{m=1}^{\infty} \frac{b_{m-1}(xe^{-c})^m}{m!}. \quad (\text{A13})$$

Equation (A13) can be rewritten as

$$(1-x)\tilde{b}(x, s) = 1 - \sum_{m=1}^{\infty} \frac{b_{m-1}(s)x^m}{m!} + s \sum_{m=1}^{\infty} \frac{b_{m-1}(s)(xe^{-c})^m}{m!}. \quad (\text{A14})$$

We now identify $x = -z/(1-z)$ and thus $z = -x/(1-x)$. Using Eq. (A14), the denominator of Eq. (A10) can be rewritten as

$$\begin{aligned} & \sum_{m=0}^{\infty} \frac{x^m}{m!} b_m(s) + \frac{xs}{1-x} \sum_{m=0}^{\infty} \frac{b_m(s)x^m}{m!(m+1)} [1 - e^{-(m+1)c}] \\ &= \tilde{b}(x, s) + \frac{xs}{1-x} \sum_{m=0}^{\infty} \frac{b_m(s)x^m}{(m+1)!} \\ & \quad - \frac{xse^{-c}}{1-x} \sum_{m=0}^{\infty} \frac{b_m(s)(xe^{-c})^m}{(m+1)!} \\ &= \tilde{b}(x, s) + \frac{s}{1-x} \sum_{m=1}^{\infty} \frac{b_{m-1}x^m}{m!} + \\ & \quad - \frac{1}{1-x} \left[(1-x)\tilde{b}(x, s) - 1 + \sum_{m=1}^{\infty} \sum_{m=1}^{\infty} \frac{b_{m-1}x^m}{m!} \right] \\ &= \frac{1}{1-x} \left[1 - (1-s) \sum_{m=1}^{\infty} \frac{b_{m-1}(s)x^m}{m!} \right]. \quad (\text{A15}) \end{aligned}$$

Reintroducing $z = -x/(1-x)$, we rewrite Eq. (A10) in a more amenable form to carry out the expansion around $s = 1$:

$$1 + a_0 = \frac{1}{(1-z) \left[1 - (1-s) \sum_{m=1}^{\infty} \frac{b_{m-1}(s)}{m!} \left(-\frac{z}{1-z} \right)^m \right]}. \quad (\text{A16})$$

By expanding a_0 in $s = 1 - \epsilon$ as $\epsilon \rightarrow 0$ we can extract the derivative of a_0 in $s = 1$. After some algebra we finally arrive at the generating function of $\langle M \rangle_N$:

$$\begin{aligned} \tilde{M}(z) &= \sum_{N=1}^{\infty} \langle M \rangle_N z^N = \left. \frac{\partial a_0}{\partial s} \right|_{s=1} \\ &= -\frac{1}{1-z} \sum_{m=0}^{\infty} \frac{b_m(1)}{(m+1)!} \left(-\frac{z}{1-z} \right)^{m+1}. \quad (\text{A17}) \end{aligned}$$

In accordance to Eq. (28), the average number of records $\langle M \rangle_N$ identifies with the coefficient z^N in the series expansion of $\tilde{M}(z)$ at $z = 0$. The explicit expression of $\langle M \rangle_N$ is given in Eq. (36).

APPENDIX B: ASYMPTOTICS OF $\langle M \rangle_N$

From now on $b_m = b_m(1)$ and $\tilde{b}(x) = \tilde{b}(x, 1)$. The behavior of $\langle M \rangle_N$ for $N \rightarrow \infty$ is hard to extract from Eq. (36). It is then

useful to restart from Eq. (A17) and introduce the function $\tilde{g}(x)$ such that

$$\tilde{M}(z) = -\frac{1}{1-z} \tilde{g} \left(-\frac{z}{1-z} \right). \quad (\text{B1})$$

The function $\tilde{g}(x)$ writes

$$\tilde{g}(x) = \sum_{m=0}^{\infty} b_m \frac{x^{m+1}}{(m+1)!}. \quad (\text{B2})$$

The asymptotics of $\langle M \rangle_N$ for large N is controlled by the behavior of $\tilde{M}(z)$ when $z \rightarrow 1$, which is equivalent to $\tilde{g}(x)$ when $x \rightarrow -\infty$. By the definition of $\tilde{b}(x)$ (A13) it is straightforward to note that

$$\frac{d\tilde{g}(x)}{dx} = \tilde{b}(x). \quad (\text{B3})$$

Setting $s = 1$ in Eq. (A14) gives

$$(1-x)\tilde{b}(x) = 1 - \sum_{m=1}^{\infty} \frac{b_{m-1}x^m}{m!} + \sum_{m=1}^{\infty} \frac{b_{m-1}(xe^{-c})^m}{m!}. \quad (\text{B4})$$

We can derive two differential equations for $\tilde{g}(x)$ and $\tilde{b}(x)$: The first is obtained by rewriting each term of (B4) using $\tilde{g}(x)$:

$$(1-x) \frac{d\tilde{g}(x)}{dx} = 1 - \tilde{g}(x) + \tilde{g}(xe^{-c}). \quad (\text{B5})$$

The second is obtained from the derivative of (B4) with respect to x :

$$\frac{d\tilde{b}(x)}{dx} = \frac{e^{-c}\tilde{b}(e^{-c}x)}{1-x}. \quad (\text{B6})$$

Note that Eq. (B6) is a first-order nonlocal differential equation. The representation of $\tilde{b}(x)$ given in Eq. (A13) is not suitable for studying the limit $x \rightarrow -\infty$. Instead the solution of (B6) gives us a nice series representation of $\tilde{b}(x)$ around $x \rightarrow -\infty$ using the following ansatz:

$$\tilde{b}(x) = \sum_{k=0}^{\infty} A_k (-x)^{-\phi-k}. \quad (\text{B7})$$

By plugging the ansatz in (B6) we find that coefficients satisfy

$$A_k = \frac{k-1+\phi}{e^{c\phi}\phi-k-\phi} A_{k-1} \quad (\text{B8})$$

with A_0 to be determined. The exponent ϕ is the solution of

$$\phi = (e^{-c})^{1-\phi}. \quad (\text{B9})$$

At most two solutions exist for (B9):

For $c < 1$ one solution is $\phi = 1$ and the other is $\phi(c) > 1$.

For $c > 1$ one solution is $\phi = 1$ and the other is $\phi(c) < 1$

For $c = 1$ the two solutions coincide, i.e., $\phi = 1$.

From now on we assume $c \neq 1$ and rewrite the ansatz (B7) in order to make explicit the existence of two solutions:

$$\tilde{b}(x) = A_0 \sum_{k=0}^{\infty} \frac{c_k}{(-x)^{\phi+k}} + B_0 \sum_{k=0}^{\infty} \frac{\tilde{c}_k}{(-x)^{k+1}}, \quad (\text{B10})$$

where

$$c_k = \prod_{m=1}^k \frac{m-1+\phi}{(e^{cm}-1)\phi-m} \quad (\text{B11})$$

and

$$\tilde{c}_k = \prod_{m=1}^k \frac{m}{e^{cm}-m-1} \quad (\text{B12})$$

with $c_0 = \tilde{c}_0 = 1$. Both c_k and \tilde{c}_k come from the iteration of Eq. (B8). To complete the solution we have to find A_0 and B_0 . Before that we note that identifying $\phi(c) = 1 - \lambda(c)$ Eq. (44) is equivalent to Eq. (B9). The case $c > 1$ corresponds to a positive $\lambda(c)$, to the existence of a stationary state and when $x \rightarrow -\infty$ to $\tilde{b}(x) \sim A_0(-x)^{-\phi}$, while when $c < 1$ no stationary state exists and $\tilde{b}(x) \sim B_0/(-x)$.

To set A_0 and B_0 we need two relations. The first relation is found by matching at $x = -1$ the value of $\tilde{b}(x)$ in the two-series representation given by (A13) and (B10):

$$\tilde{b}(-1) = \sum_{m=0}^{\infty} (-1)^m \frac{b_m}{m!} = A_0 \sum_{k=0}^{\infty} c_k + B_0 \sum_{k=0}^{\infty} \tilde{c}_k. \quad (\text{B13})$$

From the solution (B10) we can find, up to an integration constant $\mu(c)$, $\tilde{g}(x)$:

$$\begin{aligned} \tilde{g}(x) = & A_0 \sum_{k=0}^{\infty} \frac{c_k(-x)^{-\phi-k+1}}{\phi+k-1} + B_0[-\ln(-x)] \\ & + B_0 \sum_{k=1}^{\infty} \tilde{c}_k \frac{(-x)^{-k}}{k} + \mu(c). \end{aligned} \quad (\text{B14})$$

The second relation corresponds to imposing that Eq. (B14) must be a solution of (B5):

$$\begin{aligned} (1-x) & \left[A_0 \sum_{k=0}^{\infty} c_k(-x)^{-\phi-k} + B_0 \sum_{k=0}^{\infty} \tilde{c}_k(-x)^{-k-1} \right] \\ = & 1 - \left[A_0 \sum_{k=0}^{\infty} \frac{c_k(-x)^{-\phi-k+1}}{\phi+k-1} + B_0[-\ln(-x)] \right] \\ & - \left[B_0 \sum_{k=1}^{\infty} \tilde{c}_k \frac{(-x)^{-k}}{k} + \mu(c) \right] \\ & + \left[A_0 \sum_{k=0}^{\infty} \frac{c_k(-xe^{-c})^{-\phi-k+1}}{\phi+k-1} + B_0[-\ln(-xe^{-c})] \right] \\ & + \left[B_0 \sum_{k=1}^{\infty} \tilde{c}_k \frac{(-xe^{-c})^{-k}}{k} + \mu(c) \right]. \end{aligned} \quad (\text{B15})$$

B_0 comes from matching the coefficients of order $(-x)^0$:

$$B_0 = \frac{1}{1-c}. \quad (\text{B16})$$

By matching coefficients $(-x)^{-k}$ and $(-x)^{-\phi-k}$ one confirms the solution (B10). A_0 is determined using Eq. (B13):

$$A_0 = \frac{\sum_{m=0}^{\infty} (-1)^m \frac{b_m}{m!} - \frac{1}{1-c} \sum_{k=0}^{\infty} \tilde{c}_k}{\sum_{k=0}^{\infty} c_k}. \quad (\text{B17})$$

Finally we can write $\tilde{g}(x)$:

$$\begin{aligned} \tilde{g}(x) = & A_0 \sum_{k=0}^{\infty} \frac{c_k(-x)^{-\phi-k+1}}{\phi+k-1} + \frac{1}{1-c}[-\ln(-x)] \\ & + \frac{1}{1-c} \sum_{k=1}^{\infty} \tilde{c}_k \frac{(-x)^{-k}}{k} + \mu(c). \end{aligned} \quad (\text{B18})$$

The constant $\mu(c)$ is up to now undetermined and must be found by matching $\tilde{g}(x)$ at $x = -1$ with the power series representation in (B2):

$$\begin{aligned} A_0 \sum_{k=0}^{\infty} \frac{c_k}{\phi+k-1} + \frac{1}{1-c} \sum_{k=1}^{\infty} \frac{\tilde{c}_k}{k} + \mu(c) \\ = \sum_{m=0}^{\infty} \frac{b_m(-1)^{m+1}}{(m+1)!}. \end{aligned} \quad (\text{B19})$$

Having now a representation for $\tilde{g}(x)$ we can invert $\tilde{M}(z)$ by making use of Eq. (B1). For $z \rightarrow 1$ it is useful approximate the series of the generating function with a Laplace transform by setting $z = 1 - s$ in the limit $s \rightarrow 0$:

$$\sum_{N=1}^{\infty} \langle M \rangle_N z^N \approx \int dN \langle M \rangle_N e^{-sN}. \quad (\text{B20})$$

Using Eq. (B1):

$$\mathcal{L}_s[\langle M \rangle_N] = \int dN \langle M \rangle_N e^{-sN} \approx -\frac{1}{s} \tilde{g}\left(-\frac{1}{s}\right). \quad (\text{B21})$$

We now make use of two well-known inverse Laplace transforms:

$$\mathcal{L}_s^{-1}\left[\frac{1}{s^\alpha}\right] = \frac{1}{\Gamma(\alpha)} N^{\alpha-1}, \quad (\text{B22})$$

$$\mathcal{L}_s^{-1}\left[-\frac{\ln(s)}{s}\right] = \ln(N). \quad (\text{B23})$$

For $c > 1$ we find

$$\langle M \rangle_N \approx \frac{A_0}{(1-\phi)\Gamma(2-\phi)} N^{1-\phi} + \frac{1}{1-c} \ln N + O(\ln N). \quad (\text{B24})$$

For $c < 1$ we find

$$\langle M \rangle_N \approx \frac{1}{1-c} \ln N - \mu(c). \quad (\text{B25})$$

The particular values for $A_0(c)$ and $\mu(c)$ used in the main text were found with Mathematica.

What is left now is the $c = 1$ case. Since the two solutions for ϕ from (B9) coincide at $c = 1$, we need to solve for $\tilde{b}(x)$ using a different “degenerate” ansatz. In this case Eq. (B6) becomes

$$\frac{d\tilde{b}(x)}{dx} = \frac{1}{1-x} \frac{1}{e} \tilde{b}\left(\frac{x}{e}\right). \quad (\text{B26})$$

We use the following ansatz:

$$\tilde{b}(x) = \ln(-x) \sum_{k=1}^{\infty} A_k (-x)^{-k} + \sum_{k=1}^{\infty} B_k (-x)^{-k}. \quad (\text{B27})$$

The coefficients A_k satisfy

$$A_k = \frac{k-1}{e^{k-1}-k} A_{k-1} \tag{B28}$$

with A_1 undetermined. The expression of the coefficients B_k is more involved:

$$A_k(e^{k-1}-1) - B_k(e^{k-1}-1) = A_{k-1} - (k-1)B_{k-1} \tag{B29}$$

with B_1 undetermined. The function $\tilde{g}(x)$ is obtained integrating (B27). We report only the first terms:

$$\tilde{g}(x) = \mu(c) - \frac{A_1}{2} \ln^2(-x) + \dots \tag{B30}$$

By using Eqs. (B4) and (B5) we can find the undetermined coefficients as we did for the $c \neq 1$ case. By inverting the Laplace transform we thus finally obtain the leading asymptotic behavior for large N :

$$\langle M \rangle_N \approx \ln^2(N) \quad c = 1. \tag{B31}$$

APPENDIX C: EXPONENTIAL CASE: RECORD CORRELATIONS

By using Eqs. (30) and (17) we can find the correlation between two subsequent records at the stationary state. We denote by R' the record and its successive by R . First of all we compute the conditional average of R given R' . It is straightforward since we know $q(R|R')$ from Eq. (30):

$$\mathbb{E}[R|R'] = 1 + (R' - c)\theta(R' - c). \tag{C1}$$

The expected value of RR' is thus given by

$$\mathbb{E}[RR'] = \int dR' q(R') R' \mathbb{E}[R|R']. \tag{C2}$$

By substituting $q(R') = \lambda e^{-\lambda R'}$,

$$\mathbb{E}[RR'] = \frac{1}{\lambda} + \frac{(1-\lambda)}{\lambda^2} [2 - \ln(1-\lambda)]. \tag{C3}$$

By subtracting $\mathbb{E}[R]\mathbb{E}[R'] = \lambda^{-2}$ we obtain the covariance between R and R' :

$$\text{Cov}[RR'] = \frac{1-\lambda}{\lambda^2} [1 - \ln(1-\lambda)]. \tag{C4}$$

Finally the Pearson correlation coefficient takes a simple form:

$$\rho(\lambda) = \frac{\text{Cov}[RR']}{\text{Var}[R']} = (1-\lambda)[1 - \ln(1-\lambda)]. \tag{C5}$$

As $\lambda \rightarrow 1$ (or $c \rightarrow 1$) $\rho(\lambda)$ diverges and we recover the long-range correlation of the classical record process. On the other hand if $\lambda \rightarrow 0$ (i.e., $c \rightarrow \infty$) $\rho(\lambda) \rightarrow 0$ and all records become uncorrelated.

APPENDIX D: BOUNDED CASE: $P_N(M, R)$

We restrict to the case of bounded distribution in $[0,1]$ and $c \geq 1/2$. For $c \leq R \leq 1$:

$$\tilde{Q}(R) = \frac{zs(1+H)v(1-R)^{v-1}}{1-z[1-(1+c-R)^v]}, \tag{D1}$$

where we denote by $H = \int_0^1 \tilde{Q}(R') dR'$. For $1-c \leq R \leq c$,

$$\tilde{Q}(R) = zs(1+H)v(1-R)^{v-1}. \tag{D2}$$

For $0 \leq R \leq 1-c$,

$$\begin{aligned} \tilde{Q}(R) &= zs \left(1 + \int_0^{R+c} dR' \tilde{Q}(R') \right) = \\ &= zs(1+K) + zs \int_c^{R+c} dR' \tilde{Q}(R'), \end{aligned} \tag{D3}$$

where $K = \int_0^c \tilde{Q}(R') dR'$. Finally,

$$\tilde{Q}(R) = zs(1+K) + zs \int_c^{R+c} \frac{zs(1+H)v(1-R')^{v-1}}{1-z[1-(1+c-R')^v]} dR'. \tag{D4}$$

$\tilde{Q}(R)$ has a simple expression in the case of uniform distribution $v = 1$. In this case:

$$\tilde{Q}(R) = zs(1+K) - zs^2(1+H) \ln(1-zR). \tag{D5}$$

Now we need to impose self-consistently that

$$H = \int_0^1 \tilde{Q}(R) dR. \tag{D6}$$

We get

$$\frac{H}{1+H} = s(s-1) \ln[1-(1-c)z] + sz[(1-c)s+s]. \tag{D7}$$

The generating function of $P_N(M)$ is precisely H . The generating function of $\langle M \rangle_N$,

$$\tilde{M}(z) = \sum_{N=1} \langle M \rangle_N z^N, \tag{D8}$$

is obtained by deriving H by s in $s = 1$. It is easy to show that

$$\tilde{M}(z) = \frac{2-c+\ln(c)}{(1-z)^2} + \frac{z(2-c)}{(1-z)^2}. \tag{D9}$$

By expanding around $z = 0$ we recover Eq. (72).

APPENDIX E: CLASSICAL RECORDS DISTRIBUTION

In the case of classical record statistics of i.i.d. continuous random variables it is straightforward to compute the distribution of the k th record value in the limit of an infinite sequence. Equation (31) at $c = 0$ becomes a local equation with a simple solution:

$$q_k(R) = \frac{\{-\ln[1-F(R)]\}^{k-1}}{(k-1)!} f(R). \tag{E1}$$

As a reference, Eq. (E1) has been used in [13] for modeling record temperatures in the cases of exponential and Gaussian distributions.

As an explicit example, in the case of a Weibull distribution, $q_k(R)$ has a simple expression:

$$q_k(R) = \frac{\gamma}{(k-1)!} R^{\gamma k-1} e^{-R^\gamma}. \tag{E2}$$

The average record $\langle R_k \rangle_\gamma$ can be exactly computed:

$$\langle R_k \rangle_\gamma = \frac{\Gamma(k + \frac{1}{\gamma})}{(k-1)!} \rightarrow k^{1/\gamma} \quad k \rightarrow \infty. \quad (\text{E3})$$

As expected, $\langle R_k \rangle_\gamma$ grows unboundedly as $k \rightarrow \infty$.

APPENDIX F: AVERAGE RECORD

In this section we lay down a qualitative argument for estimating the average record \bar{x} as $c \rightarrow 0^+$. The equation satisfied by $q(x)$ is

$$q(x) = f(x) \int_0^c q(y) dy + f(x) \int_c^{x+c} \frac{q(y)}{1-F(y-c)} dy. \quad (\text{F1})$$

We want to extract the average value. Multiply both sides by x and integrate by x from 0 to ∞ :

$$\bar{x} = \int_0^\infty x f(x) \int_0^c q(y) dy + \int_0^\infty x f(x) \int_c^{x+c} \frac{q(y)}{1-F(y-c)} dy. \quad (\text{F2})$$

We are interested in the limit $c \rightarrow 0^+$ and we know that in this limit the typical records become large are narrow distributed. We then try to solve Eq. (F2) using the ansatz $q(x) = \delta(x - \bar{x})$ with $\bar{x} \gg c \rightarrow 0^+$

$$\bar{x} = \frac{1}{1-F(\bar{x}-c)} \int_{\bar{x}-c}^\infty x f(x) dx. \quad (\text{F3})$$

Here we used that $\int_0^c q(y) dy = 0$ since $\bar{x} > c$. We now take a derivative with respect to \bar{x} and rearranging the terms:

$$\frac{f(\bar{x}-c)}{1-F(\bar{x}-c)} = \frac{1}{c}. \quad (\text{F4})$$

Equation (F4) is an implicit equation for \bar{x} in the limit $c \rightarrow 0^+$.

If the ratio $f(x)/[1-F(x)]$ is, for large x , an increasing function of x , we expect a diverging \bar{x} as $c \rightarrow 0^+$, which is compatible with the classical record problem. Otherwise if \bar{x} vanishes as $c \rightarrow 0^+$ we do not recover the classical record case behavior, hence we expect no stationary record distribution in this case.

APPENDIX G: NUMERICAL SIMULATIONS

In this paper we employed two numerical approaches. The first is the direct simulation of c -record observables from the time series $\{x_i\}$. Starting from $R_1 = x_1$ we label the records, we count their number M and we compute the ages of the series. By repeating this process for different time series realizations we can study all the observables reported. The second method is more efficient, but can be used only if the cumulative distribution $F(x)$ is explicitly invertible. Indeed given the record value R_{k-1} , the record R_k and the age n_k can be drawn using (30) and

$$\pi(n_k | R_{k-1}) = \begin{cases} p(R_{k-1})[1-p(R_{k-1})]^{n_k-1} & R_{k-1} > c \\ \delta_{n_k,1} & R_{k-1} < c \end{cases}, \quad (\text{G1})$$

where $p(R_{k-1}) = 1 - F(R_{k-1} - c)$. In particular from Eq. (30) the k th record is given by

$$R_k = F^{-1}[u_k + (1-u_k)F(R_{k-1}-c)]. \quad (\text{G2})$$

Here u_k is a random number uniformly distributed in the interval $[0,1]$. From Eq. (G1) the k th age is 1 when $R_{k-1} < c$, otherwise is extracted from a geometric random variable.

The first method is used to simulate the stretched exponential case, while for the exponential, the Weibull and the bounded distribution we employed the second method.

-
- [1] K. N. Chandler, J. Roy. Stat. Soc. B **14**, 220 (1952).
 [2] F. G. Foster and A. Stuart, J. Roy. Stat. Soc. **16**, 1 (1954).
 [3] M. F. Neuts, J. Appl. Prob. **4**, 206 (1967).
 [4] R. W. Schorrock, J. Appl. Prob. **9**, 316 (1972).
 [5] B. C. Arnold, N. Balakrishnan, and H. N. Nagaraja, *Records* (Wiley, New York, 1998).
 [6] V. B. Nevzorov, *Records: Mathematical Theory* (American Mathematical Society, Providence, RI, 2001).
 [7] D. Gembris, J. G. Taylor, and D. Suter, *Nature (London)* **417**, 506 (2002).
 [8] D. Gembris, J. G. Taylor, and D. Suter, *J. Appl. Stat.* **34**, 529 (2007).
 [9] E. Ben-Naim, S. Redner, and F. Vazquez, *Europhys. Lett.* **77**, 30005 (2007).
 [10] D. V. Hoyt, *Climatic Change* **3**, 243 (1981).
 [11] G. W. Basset, *Climatic Change* **21**, 303 (1992).
 [12] B. Schmittmann and R. K. P. Zia, *Am. J. Phys.* **67**, 1269 (1999).
 [13] S. Redner and M. R. Petersen, *Phys. Rev. E* **74**, 061114 (2006).
 [14] G. A. Meehl, C. Tebaldi, G. Walton, D. Easterling, and L. McDaniel, *Geophys. Res. Lett.* **36**, L23701 (2009).
 [15] G. Wergen and J. Krug, *Europhys. Lett.* **92**, 30008 (2010).
 [16] A. Anderson and A. Kostinski, *J. Appl. Meteor. Clim.* **49**, 1681 (2010).
 [17] S. N. Majumdar, P. von Bomhard, and J. Krug, *Phys. Rev. Lett.* **122**, 158702 (2019).
 [18] J. Krug and K. Jain, *Physica A* **358**, 1 (2005).
 [19] J. Krug, *J. Stat. Mech.* (2007) P07001.
 [20] S.-C. Park, I. G. Szendro, J. Neidhart, and J. Krug, *Phys. Rev. E* **91**, 042707 (2015).
 [21] S.-C. Park, J. Neidhart, and J. Krug, *J. Theor. Biol.* **397**, 89 (2016).
 [22] S.-Chan Park, and J. Krug, *J. Phys. A: Math. Theor.* **49**, 315601 (2016).
 [23] H. J. Jensen, *Adv. Solid State Phys.* **45**, 95 (2006).
 [24] L. P. Oliveira, H. J. Jensen, M. Nicodemi, and P. Sibani, *Phys. Rev. B* **71**, 104526 (2005).

- [25] P. Sibani, G. F. Rodriguez, and G. G. Kenning, *Phys. Rev. B* **74**, 224407 (2006).
- [26] C. Godrèche and J. M. Luck, *J. Stat. Mech.* (2008) P11006.
- [27] S. N. Majumdar and R. M. Ziff, *Phys. Rev. Lett.* **101**, 050601 (2008).
- [28] S. N. Majumdar, *Physica A* **389**, 4299 (2010).
- [29] S. Sabhapandit, *Europhys. Lett.* **94**, 20003 (2011).
- [30] S. N. Majumdar, G. Schehr, and G. Wergen, *J. Phys. A: Math. Theor.* **45**, 355002 (2012).
- [31] Y. Edery, A. B. Kostinski, S. N. Majumdar, and B. Berkowitz, *Phys. Rev. Lett.* **110**, 180602 (2013).
- [32] C. Godrèche, S. N. Majumdar, and G. Schehr, *J. Stat. Mech.* (2015) P07026.
- [33] C. Godrèche, S. N. Majumdar, and G. Schehr, *Phys. Rev. Lett.* **117**, 010601 (2016).
- [34] P. Mounaix, S. N. Majumdar, and G. Schehr, *J. Phys. A: Math. Theor.* **53**, 415003 (2020).
- [35] P. Le Doussal and K. J. Wiese, *Phys. Rev. E* **79**, 051105 (2009).
- [36] G. Wergen, M. Bogner, and J. Krug, *Phys. Rev. E* **83**, 051109 (2011).
- [37] G. Wergen, S. N. Majumdar, and G. Schehr, *Phys. Rev. E* **86**, 011119 (2012).
- [38] B. Sabir and M. S. Santhanam, *Phys. Rev. E* **90**, 032126 (2014).
- [39] D. Challet, *Appl. Math. Fin.* **24**, 1 (2017).
- [40] F. Mori, P. Le Doussal, S. N. Majumdar, and G. Schehr, *Phys. Rev. Lett.* **124**, 090603 (2020).
- [41] B. Lacroix-A-Chez-Toine and F. Mori, *J. Phys. A: Math. Theor.* **53**, 495002 (2020).
- [42] F. Mori, P. Le Doussal, S. N. Majumdar, and G. Schehr, *Phys. Rev. E* **102**, 042133 (2020).
- [43] G. Wergen, *J. Phys. A: Math. Theor.* **46**, 223001 (2013).
- [44] C. Godrèche, S. N. Majumdar, and G. Schehr, *J. Phys. A: Math. Theor.* **50**, 333001 (2017).
- [45] D. Bonamy and E. Bouchaud, *Phys. Rep.* **498**, 1 (2011).
- [46] D. Bonamy, *Compt. Rendu. Phys.* **18**, 297 (2017).
- [47] J. Barés, D. Bonamy, and A. Rosso, *Phys. Rev. E* **100**, 023001 (2019).
- [48] S. Santucci, K. T. Tallakstad, L. Angheluta, L. Laurson, R. Toussaint, and K. J. Maloy, *Phil. Trans. R. Soc. A* **377**, 20170394 (2019).
- [49] L. Laurson, S. Santucci, and S. Zapperi, *Phys. Rev. E* **81**, 046116 (2010).
- [50] L. de Arcangelis, C. Godano, J. R. Grasso, and E. Lippiello, *Phys. Rep.* **628**, 1 (2016).
- [51] B. Alessandro, C. Beatrice, G. Bertotti, and A. Montorsi, *J. Appl. Phys.* **68**, 2901 (1990).
- [52] S. Zapperi, A. Vespignani, and H. E. Stanley, *Nature (London)* **388**, 658 (1997).
- [53] J. P. Sethna, K. A. Dahmen, and C. R. Myers, *Nature (London)* **410**, 242 (2001).
- [54] F. Colaiori, *Adv. Phys.* **57**, 287 (2008).
- [55] M. Kardar, *Phys. Rep.* **301**, 85 (1998).
- [56] D. S. Fisher, *Phys. Rep.* **301**, 113 (1998).
- [57] S. Santucci, R. Planet, K. J. Maloy, and J. Ortin, *Europhys. Lett.* **94**, 46005 (2010).
- [58] R. Planet, J. M. Lopez, S. Santucci, and J. Ortin, *Phys. Rev. Lett.* **121**, 034101 (2018).
- [59] N. Balakrishnan, K. Balasubramanian, and D. Panchapakesan, *J. Appl. Stat. Soc.* **4**, 123 (1996).
- [60] P. Bak, K. Christensen, L. Danon, and T. Scanlon, *Phys. Rev. Lett.* **88**, 178501 (2002).
- [61] J. Barés, A. Dubois, L. Hattali, D. Dalmas, and D. Bonamy, *Nat. Commun.* **9**, 1253 (2018).
- [62] R. Ballerini and S. Resnick, *J. Appl. Probab.* **22**, 487 (1985).
- [63] R. Ballerini and S. Resnick, *Adv. Appl. Probab.* **19**, 801 (1987).
- [64] K. Borovkov, *J. Appl. Probab.* **36**, 668 (1999).
- [65] J. Franke, G. Wergen, and J. Krug, *J. Stat. Mech.* (2010) 10013.
- [66] G. Wergen, J. Franke, and J. Krug, *J. Stat. Phys.* **144**, 1206 (2011).
- [67] J. Franke, G. Wergen, and J. Krug, *Phys. Rev. Lett.* **108**, 064101 (2012).
- [68] S. N. Majumdar, A. Pal, and G. Schehr, *Phys. Rep.* **840**, 1 (2020).
- [69] S. Sabhapandit and S. N. Majumdar, *Phys. Rev. Lett.* **98**, 140201 (2007).